A SEDIMENT TREND ANALYSIS (STA®) OF THE HYLEBOS WATERWAY: IMPLICATIONS TO CONTAMINANT TRANSPORT

By:

Patrick McLaren, Ph.D., P.Geo.

GeoSea® Consulting (Canada) Ltd.
789 Saunders Lane
Brentwood Bay, BC, V8M 1C5
Canada
Ph./Fax: (250) 652-1334
www.geosea.ca

August 2001

TABLE OF CONTENTS

LIST OF FIGURES

LIST OF TABLES

APPENDICES

1 INTRODUCTION

1.1 Background

On July 3, 2001, GeoSea was asked to undertake a Sediment Trend Analysis (STA®) of the Hylebos Waterway, Tacoma Harbor (Fig.1). STA is a technique that uses the complete grain-size distributions of the bottom sediments to determine the net transport pathways of the sediments together with their dynamic behavior (i.e., accretion, erosion, dynamic equilibrium etc.). Because many contaminants associate with particles that make up the natural sediment, this information may be used directly to assess the relationship between contaminant loadings and their sources, as well as the fate and behavior of contaminants that may be contained in the sediments.

The purpose of this work, therefore, is to map in detail the sediment types present in the waterway and, using STA, determine their transport pathways and dynamic behavior. In addition, this information is examined and correlated with present contaminant levels and used to assess their relationship with known sources.

The original theory that is required to carry out STA was first published in McLaren and Bowles (1985). Since that time, however, there have been various refinements, particularly on the ability to determine transport pathways over two dimensions. A short summary of the theory is contained in Section 2.0 (to allow most readers to follow the findings of the report), and a full, recently revised version of the mathematics and derivation of sediment trends is provided in Appendix I.

1.2 Objectives

The specific objectives of the STA are to:

(1) Collect about 240 sediment grab samples from the bed of the Hylebos Waterway.

(2) Analyze all samples for their complete grain-size distribution and establish, using the technique of STA, the present patterns of transport, and areas of erosion, stability (dynamic equilibrium) and deposition.

(3) Define specific "transport environments" based on sediment characteristics and their dynamic behavior.

(4) Correlate the derived patterns of transport with known processes and/or modeling studies.

(5) Use the above findings to advise on the probable extent of contamination from specific sources.

1.3 Field Methods

Sediment grab samples were collected during the period July 12 –15, 2001 using a Van Veen type grab sampler. This device samples the top 10 to 15 cm of sediment. All samples were collected from a 12-foot, hard-bottom inflatable speedboat (Caribe) equipped with a depth sounder, a small electric winch, and grab sampler. Positions were

obtained using a differential Global Positioning System (GPS) receiver with 2 m accuracy in differential mode (Trimble DS212L). In most instances, samples were obtained at predetermined locations; however, where shoreline structures (e.g. docks and marinas) and vessels interfered with navigation, samples were collected as close as practicable to the planned position. Representative samples from each successful grab were stored in plastic bags and transported to the GeoSea laboratory in Brentwood Bay, BC, for grain-size analyses.

Samples were collected on a regular hexagonal grid with a spacing of 110m in the outer portion of the Waterway (from Commencement Bay to the start of the Lower Turning Basin) and 55 m to include the Lower Turning Basin landwards to the Upper Turning Basin (Fig.1). A total of 251 sample sites were visited, of which 9 were found to be "hard ground" (usually occurring when a bark mulch covered the bottom) and no sample could be taken. A site was designated as hard ground after three separate drops of the grab sampler failed to retrieve sediment. Various qualitative observations were recorded at the time of sampling including sediment color, smell, the presence of biota, wood debris etc. These observations are in the data base and available to be mapped on the GIS. An example map is shown in Figure 2.

1.4 Grain-Size Analysis

All samples were analyzed for their complete grain-size distribution using a Malvern MasterSizer 2000 laser particle sizer. The laser-derived distributions were combined with sieve data for sizes >1500 microns using a merging algorithm developed by GeoSea Consulting[1]. The distributions were entered into a computer equipped with proprietary software to establish sediment trends and transport functions. A more complete description of the grain-size analytical technique is provided in Appendix II.

2 THEORY

The technique to determine the sediment transport regime utilizes the relative changes in grain-size distributions of the bottom sediments. The derived patterns of transport are, in effect, an integration of all processes responsible for the transport and deposition of the bottom sediments. The latter may be considered as a facies that is defined by its grain-size distribution. Details of the theory are described in Appendix I; however, the approach is summarized here.

Suppose two sediment samples (D_1 and D_2)[2] are taken sequentially in a known transport direction (for example from a river bed where D_1 is the up-current sample and D_2 is the

---

[1] The grain-size data (listed in Appendix II) are supplied on a disk as an Excel worksheet containing sample locations and the complete phi distributions of the sediments.

[2] A sample is considered to provide a representation of a sediment type (or facies). There is no direct time connotation, nor does the depth to which the sample was taken contain any significance (provided, of course, that the sample does, in fact, accurately represent the facies). For example, D_1 may be a sample of a facies that represents an accumulation over several tidal cycles, and D_2 represents several years of deposition. The trend analysis simply provides the sedimentological relationship between the two. It is

down-current sample). The theory shows that the sediment distribution of D_2 may become finer (Case B) or coarser (Case C) than D_1: if it becomes finer, the skewness of the distribution must become more negative. Conversely, if D_2 is coarser than D_1, the skewness must become more positive. The sorting will become better (i.e., the value for variance will become less) for both Case B and C. If either of these two trends is observed, we can infer that sediment transport is occurring from D_1 to D_2. If the trend is different from the two acceptable trends (e.g. if D_2 is finer, better sorted and more positively skewed than D_1), the trend is unacceptable and we cannot suppose that transport between the two samples has taken place.

In the above example, where we are already sure of the transport direction, $D_2(s)$ can be related to $D_1(s)$ by a function X(s) where 's' is the grain size. The distribution of X(s) may be determined by:

$$X(s)= D_2(s)/D_1(s)$$

X(s) provides the statistical relationship between the two deposits and its distribution defines the relative probability of each particular grain size being eroded, transported and deposited from D_1 to D_2.

2.1 Interpretation of Dynamic Behavior

The shape of X(s) when compared to the D_1 and D_2 distributions (Fig.A-6; Appendix I) provides the following six interpretations on the dynamic behavior of the sediments. All six dynamic behaviors were present in the Hylebos Waterway study. They are as follows:

(1) Net Accretion: The shapes of the three distributions are similar, but the mode of X is finer than the modes of D_1 and D_2. Sediment must fine in the direction of transport; however, more fine grains are deposited along the transport path than are eroded, with the result that the bed, though mobile, is accreting.

(2) Net Erosion: Again the shapes of the three distributions are similar, but the mode of X is coarser than the D_1 and D_2 modes. Sediment coarsens along the transport path, more grains are eroded than deposited, and the bed is undergoing net erosion.

(3) Dynamic Equilibrium: The shape of the X-distribution closely resembles the D_1 and D_2 distributions. The relative probability of grains being transported, therefore, is a similar distribution to the actual deposits. This suggests that the probability of finding a particular grain in the deposit is equal to the probability of its transport and re deposition (i.e., there is a grain by grain replacement along the transport path). The bed is neither accreting nor eroding and is, therefore, in dynamic equilibrium.

---

unable to determine the rate of deposition at either locality, but frequently the derived patterns of transport do provide an indication of the probable processes that are responsible in producing the observed sediment types.

(4) Mixed Case: This occurs when the sediment trend statistics are significant for both Net Accretion and Net Erosion (i.e., fining and coarsening trends are both statistically significant in the same direction down the transport path). It is interpreted in a similar fashion to Dynamic Equilibrium.

(5) Total Deposition (I): Regardless of the shapes of D_1 and D_2, the X-distribution more or less increases monotonically over the complete size range of the deposits. Sediment must fine in the direction of transport; however, the bed is no longer mobile. Rather, it is accreting under a "rain" of sediment that fines with distance from source. Once deposited, there is no further transport.

(6) Total Deposition (II): Recently, a fifth form of the X-distribution has been discovered. Occurring only in extremely fine sediments when the mean grain-size is very fine silt or clay, the X-distribution may be essentially horizontal (Fig.A6-E). Such sediments are usually found far from their source (compared with Deposition (I) sediments in which size-sorting of the fine particles is taking place, and therefore the source is relatively close). The horizontal nature of the X-distribution suggests that their deposition is no longer related strictly to size sorting. In other words, there is now an equal probability of all sizes being deposited. This form of the X-distribution was first observed in the muddy deposits of a British Columbia fjord and is described in McLaren, et al., 1993.

2.2 Interpretation of a Trend

In reality, a perfect sequence of progressive changes in grain-size distributions is seldom observed in a line of samples, even when the transport direction is clearly known. This is due to complicating factors such as variation in the grain-size distributions of source material, local and temporal variability in the X(s) function, and a variety of sediment sampling difficulties (i.e., sample doesn't adequately describe the deposit; it's taken too deeply; not deep enough etc.).

Initially, a trend is easily determined using a statistical approach whereby, instead of searching for "perfect" changes in a sample sequence, all possible pairs contained in the sequence are assessed for possible transport direction. When one of the trends exceeds random probability within the sample sequence, we infer the direction of transport and calculate X(s). The precise statistical technique is described more fully in Appendix I.

Despite the initial use of a statistical test, various other qualitative assessments must be made in the final acceptance or rejection of a trend. Included is an evaluation of R^2, a multiple linear correlation coefficient defining the relationship among the mean, sorting and skewness in the sample sequence. If a given sample sequence follows a transport path perfectly, R^2 will approach 1.0 (i.e., the sediments are perfectly "transport-related"). A low R^2 may occur, even when a trend is statistically acceptable for the following reasons: (i) sediments on a presumed transport path are, in reality, from different facies, and valid trend statistics occurred accidentally; (ii) the sediments are from a single facies, but the chosen sequence is only a poor approximation of the actual transport path, and (iii) extraneous sediments have been introduced into the natural transport regime, as in the case of dredged material disposal. R^2, therefore, is assessed qualitatively, and when low, statistically accepted trends must be treated with caution.

To analyze for sediment transport directions over 2-dimensions, a grid of samples is required. Each sample is analyzed for its complete grain-size distribution and these are entered into a microcomputer equipped with appropriate software to "explore" for statistically acceptable trends. The technique to explore for transport pathways is initially undertaken randomly[3] (i.e., up and down the river, across the river, lines of samples running east-west, north-south etc.). As familiarity with the data increases, exploration becomes less and less random until a single and final coherent pattern of transport is obtained[4]. On completion of an interpretation, each transport line may then be used to derive a corresponding X-function from which the behavior of the bed material on the transport path is inferred.

3 PHYSICAL SETTING

The Hylebos is the northernmost of several waterways that make up Tacoma Harbor. Extending from Commencement Bay, it runs southeast for about three miles and is generally less than 700 feet across. A small creek (Hylebos Creek) enters the Waterway at its extreme southeast end. The waterways themselves are constructed in old channels of the former Puyallup River delta, which now flows into Commencement Bay through the Puyallup Waterway. Although considerably changed by twentieth century industrialization, the river still carries an active sediment load that is presently forming a delta at its mouth in Commencement Bay. Its suspended load is quite clearly visible in the Bay and, at the time of sampling for this report, was seen to extend far into the Hylebos Waterway. Drogue studies have shown that there is a net inflow of saline water below 6m, and a net outflow at 2 to 6m. The surface also displays a net inflow, although wind from the southeast can reverse this (Loehr et. al., 1981).

With the exception of some tidal flats on the north side of the outer portion of the Hylebos Waterway, it is essentially contained in docks and shoreline structures associated with an extensive industrial complex that lines its banks (Fig.2). Because of past contaminant releases into the area, in the early 1980's Tacoma Harbor was declared a Superfund Site.

---

[3] The term "random" is used loosely in that it is not strictly possible to remove the element of human decision-making entirely. The important aspect of the initial search for sediment trends is that it is undertaken with no preconceived concept of transport directions. It is, however, assumed that there will be a net sediment transport pattern and that changes in the grain-size distributions throughout the study area will not be random. The derivation of the final patterns may be likened to communication theory which, in the case of extremely noisy signals, requires the "discovery" of a "message" as the proof that the message does indeed exist.

[4] At present, the approach of obtaining the final derivation of the net sediment transport pathways relies on assessing and removing "noise" qualitatively. The GeoSea trend programming is specifically designed to do this in that all sample distributions may be readily compared with one and other (and excessively noisy distributions discarded), the best sediment types can be determined for the analysis, and the relationships among all the sample pairs may be assessed. Because we are unable to know the exact nature of the "noise" that we may be confronted with, it is difficult at this stage to devise a quantitative technique to eliminate it. To do so is the subject of much on-going research both by GeoSea and at various universities.

4 PATTERNS OF SEDIMENT TRANSPORT

As seen from Figure 3 and Table 1 the sediments obtained from the study area range from sandy gravel to mud, with the largest proportion (57%) being sandy mud. The latter sediment type is common throughout the Waterway. The large tidal flat and shallows immediately outside the Waterway is sand, otherwise this sediment type is found at relatively random locations. Significant patches of mud are found in both the Lower and Upper Turning Basins.

SEDIMENT TYPE[5]	NO of SAMPLES	PERCENTAGE
Gravel	0	0
Sandy gravel	1	0
Gravely sand	5	2
Sand	18	7
Muddy sand	39	16
Sandy mud	143	57
Mud	33	13
Other (mixtures)	3	1
Hard Ground	9	4
TOTAL	251	100.0

Table 1: Summary of sediment types

The best patterns of transport that could be derived were possible only when all samples were used in a single interpretation (i.e., all the samples were treated as a single facies). Because the range of sizes present in each of the samples throughout the study area is relatively constant, the assumption that they are indeed all "transport-related" and can be treated as a single facies is probably correct.

Following the calculation of numerous sample sequences to determine significant trends, a total of 35 lines were selected to provide a pattern of transport (Fig.5). The trend statistics for each line are provided in Appendix III, in which it is seen that the R^2 values are nearly all exceptionally high (>0.9). Representative X-distributions[6] to illustrate the dynamic behavior derived from sample lines are referenced in Table 2, and their graphs are shown in Appendix IV. The net sediment transport pathways are shown in (Fig.6). For ease of discussion, the sample lines have been grouped into various areas (or Transport

---

5 The sediment types use 20% and 50% as "cut-off" limits. For example, sand has less than 20% of any other size; sandy mud has greater than 20% sand, but less than 50%; muddy sand has greater than 20% mud, but less than 50%; etc. The few sediments containing three modes (i.e., a muddy, sandy gravel) although obviously "noisy" distributions, were still successfully included in the STA.

[6] An X-distribution is a function derived from the grain-size distributions contained in a sample line. It is used to describe the dynamic behavior of the sediments along the transport pathway defined by the sample line. The X-distribution may be thought of as a function that describes the relative probability of each particle being removed from an "up-current" sediment sample, and being deposited in a "down-current" sample. The shape of the X-distribution relative to the distributions of the sediments making up the sample line is used to define dynamic behavior (see Fig.AI-6).

Environments; Fig.7) and described in Table 2. A Transport Environment is defined as an area within which transport lines are associated both geographically and "behaviorally". Generally, transport lines cannot be continued from one TE into another, and so a region in which transport lines naturally end (and begin) is a boundary between Transport Environments.

TABLE 2

SUMMARY OF THE SEDIMENT TRANSPORT LINES IN THE HYLEBOS WATERWAY

	Transport Environment (Fig.7)	Lines (see Fig.5)	No. of Sample Lines	R2 Values		Notes	Representative X-distributions (See Appendix IV)
				Mean	S.D.		
1	Commencement Bay	1 to 10	10	0.89	0.22	This Transport Environment is confined to Commencement Bay. There was no evidence that the samples making up this environment could be related to the sediments found immediately inside the Hylebos Waterway. This environment is composed of relatively few samples and should be accepted with caution. The trends suggest that this part of Commencement Bay is under the influence of a clockwise gyre, with the sediments originating from shoreline glacial deposits on the north side of the Bay. The nearshore trends show Net Erosion suggesting that fore-shore lowering with consequent coastal erosion is likely occurring. In the offshore deeper waters, sediments in the gyre fine to muddy sediments and Total Deposition - Type I is occurring. The relationship between this Transport Environment with TE2 (Outer Waterway) indicates that the mouth of the Hylebos is a sediment parting zone, a site where sediment must periodically be deposited prior to moving both back out into Commencement Bay, and into the Waterway. Such events are likely to be related to storm activity that brings new sediment from the shoreline to the entrance of the channel.	App.IV - Fig.1 (Line 3) App.IV - Fig.2 (Line 7)
2	Outer Waterway	11 to 19	9	0.96	0.03	These lines originate at the entrance to the Waterway and extend all the way to last bend (slightly more than one half its length). Of the 9 lines making up this environment, 7 are in Dynamic Equilibrium or Mixed Case. Such a finding is relatively rare in muddy sediments which, because of their cohesive properties, tend to form deposits of Total Deposition. The finding of Dynamic Equilibrium suggests that there are processes capable of resuspending the muddy sediments enabling transport to continue up the Waterway. A likely process causing resuspension is propeller wash. One line close to shore on the north side (Line 13) is contained in relatively coarse sediments (Fig.4) and shows Net Erosion. Line 18, on the south side and close to shore shows Total Deposition. Possibly propeller wash is less likely to affect the sediments close to, or under the pilings making up the docks in this area.	App.IV - Fig.3 (Line 17) App.IV - Fig.4 (Line 13) App.IV - Fig.5 (Line 18)

TABLE 2 (con't)

SUMMARY OF THE SEDIMENT TRANSPORT LINES IN THE HYLEBOS WATERWAY

	Transport Environment (Fig.7)	Lines (see Fig.5)	No. of Sample Lines	R2 Values Mean	R2 Values S.D.	Notes	Representative X-distributions (See Appendix IV)
3	Middle Waterway	20 to 26	7	0.94	0.06	Originating in a slightly narrower part of the Waterway, these lines continue with transport up the channel and terminate in the mud associated with the Lower Turning Basin. Except for Lines 20 and 21 on the north side of the channel which contains some sand deposits and shows Net Erosion, all the remaining lines show Total Deposition - Type I dynamic behavior. Unlike the sediments in the Outer Waterway (TE2), these sediments appear to be less susceptible to resuspension events. There are three probable reasons for this. First, the sediment has become finer and is therefore more cohesive than the sediments in the Outer Waterway; second, there may be less shipping activity with increasing distance from the mouth of the Waterway; and third, currents are known to decrease farther up the Waterway.	App.IV - Fig.6 (Line 20) App.IV - Fig.7 (Line 24)
4	Inner Waterway	27 to 34	8	0.84	0.12	Commencing in the narrows up-channel from the Lower Turning Basin, these lines continue with landward transport into the mud of the Upper Turning Basin. With the exception of Line 27 on the north side which show Total Deposition - Type I behavior, the remaining lines all produced X-distributions indicative of Total Deposition - Type II. Such behavior suggests that much of the coarser sizes in the channel have already been deposited, undoubtedly in the Lower Turning Basin, and the remaining sizes left to continue up-channel are extremely fine (i.e., there is an equal probability of all remaining sizes to be deposited.	App.IV - Fig.8 (Line 27) App.IV - Fig.9 (Line 31)
5	Hylebos Creek	35	1	1.00	-	This single line of samples taken in Hylebos Creek shows coarse sediment in Dynamic Equilibrium flowing towards the Upper Turning Basin. The influence of the creek does not appear to be particularly significant with respect to sedimentation in the Waterway.	App.IV - Fig.10 (Line 35)

5 DISCUSSION

5.1 Process Implications

The derived patterns of net sediment transport for the Hylebos Waterway show movement entirely in an up-channel direction despite considerable efforts to find reversals, or a more complex pattern within the Waterway. Furthermore, the dynamic behavior of the transport regime changes in a regular way from Dynamic Equilibrium in TE2 (Outer Waterway), followed by Total Deposition – Type I in the sediments associated with the Lower Turning Basin (Middle Waterway; TE3), and ending with extremely fine sediments in Total Deposition – Type II in TE4 (Inner Waterway). This progressive change in dynamic behavior suggests that sediments become increasingly finer (and increasingly cohesive) towards the upper end of the Waterway together with a decrease in current velocities. The latter is reported in Norton and Barnard (1992) in which velocities at the mouth were up to 10 cm sec^{-1} compared with at the head where they were generally less than 2 cm sec^{-1}. Floyd and Snider Inc. (1998) described the presence of underlying dense water masses that move regularly into the Hylebos Waterway as a result of upwelling from Commencement Bay. A similar stratification was observed by Loehr et. al. (1981) in which flood tidal currents prevailed near the bottom and surface, with a mid-layer favoring the ebb. Both current velocities and the stratification can be disturbed by vessel activities inducing mixing and possible scour (Floyd and Snider, 1998).

It is quite likely that the observed changes in dynamic behavior towards the head is also influenced by a decreasing number of vessel passages in the channel (i.e., given that docks line most of the channel, more vessels can be expected to pass back and forth in TE2 (Outer Waterway) creating conditions favorable for resuspension and Dynamic Equilibrium than in TE's 3 and 4 where Total Deposition prevails). Such resuspension events in TE3 may provide an opportunity for further transport from TE3 into TE4, after which there is no further area for sediment to be transported regardless of vessel traffic.

It is interesting that sediments in TE1 (Commencement Bay) could not be related by transport to sediments in the Waterway. In other words, there must be a significant source present in the Waterway that is not as important in the Commencement Bay environment. There are two possible explanations that are probably both operating. The first is that suspended sediment associated with the Puyallup River plume, while negligible compared with the source of sediments that are provided by a lowering foreshore along the north side of Commencement Bay, becomes a significant sediment input once inside the Waterway. Second, industrial activity and the presence of various outfalls are likely contributing a miscellany of sediment types unique to the Waterway (note that many of the isolated patches of coarse and mixed sediments are found along its banks; Fig. 4).

5.2 Implications for Contaminants

The following relationships between contaminants and sediment transport pathways were first described by McLaren (1987).

(1) Given a greater surface area and more sites available for adsorption, contaminants have a greater association with fine sediment (silt and clay) than with coarse

sediment (sand). Deposition of contaminated sediments, therefore, might be expected to increase towards the head of the Waterway with the highest concentrations associated with the mud deposits found in the two turning basins.

(2) In environments undergoing Net Accretion (Fig. A1-6B; Appendix I) there is a general linear increase of contaminant concentrations along the transport path.

(3) Contaminant loadings decrease rapidly with Net Erosion (Fig. A1-6C; Appendix I). Contaminant monitoring in such an environment will not provide useful results.

(4) Sediments in Dynamic Equilibrium (Fig. A1-6A; Appendix I) or Mixed Case show no relationship between contaminant concentrations and distance along a transport path. Contaminant levels in such environments are likely to be random and changeable.

(5) In environments of Total Deposition (I) (Fig. A1-6D; Appendix I), contaminants are generally found as localized "highs" that can usually be associated with a specific source.

(6) When the X-distribution is horizontal (Total Deposition II; Fig. A1-6E), all particles, whether contaminated or not, have an equal probability of deposition. There is not, therefore, any preferred area for the deposition of contaminants and more or less equal concentrations are to be expected throughout such an environment.

According to the above concepts, it is instructive to consider the probable behavior of contaminated particles in the Waterway *in the absence of local contaminant sources*. Assume a source of contaminated particles enters the Waterway at its mouth. The first environment encountered (TE2; Outer Waterway) is predominantly in Dynamic Equilibrium. Contaminated particles deposited in this environment will have an equal probability of continuing up-channel transport as on a conveyor belt. Hot spots might develop at random, but will tend to disperse given sufficient time. A possible hotspot that would be unlikely to disperse could form on the south side of the outer portion of this Transport Environment (along Line 18; Fig. 5).

The conveyor belt form of transport ends at the start of TE3 (Middle Waterway), an environment dominated by Total Deposition – Type I. Here, contaminated particles will come out of transport to form one or more hotspots that are unlikely to be easily dispersed. Thus the Lower Turning Basin would be expected to be an important contaminant sink.

Finally, TE4 (Inner Waterway) is dominated by Total Deposition – Type II, an environment where the remaining particles in transport are sufficiently fine that they "escaped" deposition in the Lower Turning Basin, and they now have an equal probability of deposition anywhere in the Upper Turning Basin. Specific hotspots would be unlikely; however, a ubiquitous contaminant level throughout the environment would more probably be observed. It is emphasized that throughout all three of the Hylebos Transport Environments, it would be very unlikely for a contaminated particle to have the opportunity to move in the reverse direction towards the mouth.

In reality, the high level of industry surrounding the Waterway has resulted in numerous contaminant sources. Like sediment, the greater the amount of contaminant entering the environment, the greater the probability of its deposition in the sediment *regardless of the dynamic behavior*. For example, a significant contaminant source in TE2 (Outer Waterway) where the sediments are predominantly in Dynamic Equilibrium may well form local hotspots by simply overwhelming the sedimentary environment. Although the hotspot may be dispersed in the up-channel direction, without an effective source control program, the original hotspot will be continually replenished.

In order to relate the findings of the STA with known contaminant levels, a contaminant database was provided to GeoSea (from Striplin and Associates). Because of the large size of the database, and the extensive number of organic and heavy metals available, it was necessary to make various practical decisions. The database was edited to include only surface samples; thus sample identities ending in 'A', 'B' or 'C' which were assumed to be from cores were not used in the analysis. Any samples whose identifiers did not end in 'A', 'B' or 'C' were assumed to be either surface samples or intertidal and were used in the analysis. Some data collected during particular surveys were not described well enough in the provided documentation to be used with confidence. Therefore, only values from the following data sets were used: Events 1A and 1C, grab and intertidal samples only; Event 1C Phase 2; Event 1C April 1996; and, Round 2, Phases I and II. Any data values with codes 'J' or 'U' (estimated or not detected) were also excluded, with the result that none of the data for volatiles was examined.

Numerous maps of various contaminants were constructed with the aid of Surfer®, a contouring and 3D surface mapping software package made by Golden Software, Inc. It was found that separate maps of the organic compounds generally produced similar patterns, as did separate maps of the trace metals data. For this reason, it was decided to examine only two maps, namely Total Organics (essentially pesticides and PCB's; Fig. 8) and Total Trace Metals (An, As, Cd, Cr, Cu, Pb, Hg, Ni, Ag, and Zn; Fig.9).

The relationship between the Transport Environments and Total Organics is excellent (Fig.8). In TE2 (Outer Waterway), there are several isolated hotspots (shown as A, B, C and D on Figure 8). Not all the hotspots are necessarily related to an immediate shoreline source (e.g., hotspots B and C), and these may well constitute random locations in an environment of Dynamic Equilibrium where the contaminants are contained within a sediment conveyor belt moving towards the head of the Waterway. The most intense hotspot is D, which seems likely to be related to a specific shoreline source. Hotspots E, F, G and H are nearly all out in mid-channel (i.e., no immediate shoreline source) and appear relatively isolated as expected in an environment of Total Deposition – Type I. Finally, Transport Environment 4 (Inner Waterway) shows a more or less equal spread of values throughout, which is also expected in an environment of Total Deposition – Type II.

An examination of the distribution of total metals (Fig.9) reveals 4 significant hotspots that are clearly related to shoreline sources. Hotspots A, B and D fall on transport pathways of Total Deposition – Type I and they may be stable at these positions. Unlike the map for total organics, no metal hotspots are present in the Lower Turning Basin, and the values found here are much the same as those in the Upper Turning Basin. Possibly

the metals associate with finer size fractions than the organics, thereby making their dispersal somewhat more random. There are also far fewer samples for the metals (192 compared with 330 organic samples), which may be a factor in simply failing to find as many hotspots.

6 SUMMARY AND CONCLUSIONS

(1) A Sediment Trend Analysis was performed using 242 sediment samples taken from the Hylebos Waterway. Qualitative descriptions were made of each sample including color, smell, biota and wood debris, all of which are included in the GIS accompanying this report. Most of the samples (57%) are sandy mud, although sediments generally fine in the channel from its mouth to its head. Significant patches of mud are located in each of the two Turning Basins. All samples were used as a single facies to derive the sediment trends.

(2) Thirty-five sample sequences (lines) were selected to show the best possible transport pathways and these divided up into five distinct Transport Environments (Te's) extending from the mouth to the head of the Waterway

(3) The STA revealed that sediments immediately outside the Waterway in Commencement Bay are separate from those inside the Waterway. This is explained by the dominance of a shoreline source along the north shore of Commencement Bay, most of which does not enter the Waterway. The latter contains sediments from a variety of shoreline sources (often due to industrial activities) as well as fine sediment input from the Puyallup River plume. It is the combination of these two sources that causes the Waterway sediments to be uniquely different to those in Commencement Bay.

(4) The trends inside the Waterway all showed net sediment movement towards its head. The dynamic behavior changed progressively from Dynamic Equilibrium in the Outer Waterway (TE2), to Total Deposition – Type I behavior in the Middle Waterway (TE3) to Total Deposition – Type II in the Inner Waterway (TE4). These findings correspond well with known processes in which flood currents dominate and are stronger nearer the mouth than the head of the Waterway.

(5) Vessel traffic is likely helpful in resuspending sediment in TE2 resulting in Dynamic Equilibrium as well as enabling some further movement from TE 3 into TE4. If sediments were disturbed by propeller wash in TE4, they would likely remain in that environment.

(6) The sediment trends suggest that, in the event of a contaminant entering the waterway and becoming associated with the sediments, its movement towards the mouth would be extremely unlikely compared with its movement towards the head.

(7) The dynamic behavior of TE2 suggests that contaminant hotspots would be random and, in the long term, ephemeral as they move in a conveyor belt fashion towards the head of the Waterway. In TE3 hotspots are likely to form and remain stationary, with little or no further movement, whereas in TE4 hotspots would be less likely. Instead contaminant levels are would be relatively evenly distributed over the entire area of the Transport Environment.

(8) The relationships described in (7) are somewhat obscured by the presence of significant shoreline sources of contaminants evidently entering the Waterway. At such places the abundance of the source can, at least temporarily, overwhelm the effects of the existing dynamic behavior of the receiving sediments. Nevertheless, maps of total organic contaminants and total trace metals correlate remarkably well with the Transport Environments defined by the STA.

7 REFERENCES

Floyd & Snider Inc., 1998: Circulation, water properties, and ship-induced scour. Hylebos Waterway Wood Debris Program, Events 1A and 1B Data Report, Agency Draft, 7/8/98.

Loehr, L.C., Collias, E. C., Sullivan, R. H., and Haury, D., 1981: Commencement Bay studies technical report, Vol. VI, Physical Oceanography, prepared by Dames & Moore for the U.S. Army Corps of Engineers, Seattle District.

McLaren, P., and Bowles, D., 1985: The effects of sediment transport on grain-size distributions. Journal of Sedimentary Petrology, 55, 457-470.

McLaren, P., 1987: The effects of sediment transport on contaminant dispersal: an example from Milford Haven, Wales. Marine Pollution Bulletin, 18, 586-594.

McLaren, P., Cretney, W.J., and Powys, R.I.L., 1993: Sediment pathways in a British Columbia fjord and their relationship with particle-associated contaminants. Journal of Coastal Research, 9, 1026-1043.

Norton, D., and Barnard, R., 1992: Spatial and temporal trends in contaminant levels in settling particulate matter: Hylebos Waterway (Commencement Bay), July 1990 to November 1991. Washington State Department of Ecology, Environmental Investigations and Laboratory Services Program, Toxic Compliance and Ground Water Monitoring Section. Water Body No. WA-10-0020 (Segment No. 05-10-01). 43 p + Appendices.

APPENDIX I

Sediment Transport Model

TABLE OF CONTENTS

LIST OF FIGURES

LIST OF TABLES

1 SEDIMENT TRANSPORT MODEL

The following is a brief review of the sediment transport model, a detailed analysis of which is contained in McLaren and Bowles (1985). The required information used throughout this analysis is the grain-size distribution which, for the purpose of Sediment Trend Analysis, is defined for any size class as the probability of the sediment being found in that size class. Size classes are defined in terms of the well-known ϕ (phi) unit, where d is the effective diameter (diameter of the sphere with equivalent volume) of the grain in millimeters.

$$d(\text{mm}) = 2^{-\phi}\ ;\ \text{or}\ \log_2 d(\text{mm}) = -\phi \quad \text{.....(1)}$$

Given that the grain-size distribution $g(s)$, where s is the grain size in phi units, is a probablility distribution, then

$$\int_{-\infty}^{\infty} g(s)ds = 1 \quad \text{.....(2)}$$

In practice, grain-size distributions do not extend over the full range of s, and are not continuous functions of s. Instead we work with discretized versions of $g(s)$ with estimates of $g(s)$ in finite sized bins of 0.5ϕ width.

Three parameters related to the first 3 central moments of the grain-size distribution are of fundamental importance in Sediment Trend Analysis. They are defined here, both for a continuous $g(s)$ and for its discretized approximation with N size classes. The first parameter is the mean grain size (μ), defined as:

$$\mu = \int_{-\infty}^{\infty} s \cdot g(s)ds \approx \sum_{i=1}^{N} s_i \cdot g(s_i) \quad \text{.....(3)}$$

The second parameter is sorting (σ) which is equivalent to the variance of the distribution, defined as:

$$\sigma^2 = \int_{-\infty}^{\infty} (s-\mu)^2 \cdot g(s)ds \approx \sum_{i=1}^{N} (s_i-\mu)^2 \cdot g(s_i) \quad \text{.....(4)}$$

Finally, the coefficient of skewness (κ) is defined as:

$$\kappa = \frac{1}{\sigma^3} \int_{-\infty}^{\infty} (s-\mu)^3 \cdot g(s)ds \approx \frac{1}{\sigma^3} \sum_{i=1}^{N} (s_i-\mu)^3 \cdot g(s_i) \quad \text{.....(5)}$$

1.1 Case A (Development of a lag deposit)

Consider a sedimentary deposit that has a grain-size distribution $g(s)$ (Figure AI- 1). If eroded, the sediment that goes into transport has a new distribution, $r(s)$, which is derived from $g(s)$ according to the function $t(s)$ so that:

$$r(s_i) = k \cdot g(s_i)t(s_i)$$

$$\text{or} \quad t(s_i) = \frac{r(s_i)}{k \cdot g(s_i)} \qquad \text{.....(6)}$$

where $g(s_i)$ and $r(s_i)$ define the proportion of the sediment in the i[th] grain-size class interval for each of the sediment distributions. k is a scaling factor[1] that normalizes $r(s)$ so that:

$$\sum_{i=1}^{N} r(s_i) = 1$$

$$\text{thus} \quad k = \frac{1}{\sum_{i=1}^{N} g(s_i)t(s_i)} \qquad \text{.....(7)}$$

With the removal of $r(s)$ from $g(s)$, the remaining sediment (a lag) has a new distribution denoted by $l(s)$ (Figure AI- 1) where:

$$l(s_i) = k \cdot g(s_i)[1 - t(s_i)]$$

$$\text{or} \quad t'(s_i) = \frac{l(s_i)}{k \cdot g(s_i)} \qquad \text{.....(8)}$$

$$\text{where} \quad t'(s_i) = 1 - t(s_i)$$

The function $t(s)$ is defined as a sediment transfer function and is described in exactly the same manner as a grain-size probability function except that it is not normalized. It may be thought of as a function that incorporates all sedimentary and dynamic processes that result in initial movement and transport of particular grain sizes.

Data from flume experiments show that distributions of transfer functions change from having a high negative skewness to being nearly symmetrical (although still negatively skewed) as the energy of the eroding/transporting process increases. These two extremes in the shape of $t(s)$ are termed low energy and high energy transfer functions respectively (Figure AI- 2). The shape of $t(s)$ is also dependent, not only on changing energy levels of the process involved in erosion and transport, but also on the initial distribution of the original bed material, $g(s)$(Figure AI- 1). The coarser $g(s)$ is, the less likely it is to be acted upon by a high energy transfer function. Conversely, the finer $g(s)$ is, the easier it becomes for a high energy transfer function to operate on it. In other words, the same process may be represented by a high energy transfer function when acting on fine sediments, and by a low energy transfer function when acting on coarse sediments. The terms high and low energy are, therefore, relative to the distribution of $g(s)$ rather than to the actual process responsible for erosion and transport.

---

[1] 'k' is actually more complex than a simple normalizing function, and its derivation and meaning is the subject of further research. It appears to take into account the masses of sediment in the source and in transport, and may be related to the relative strength of the transporting process.

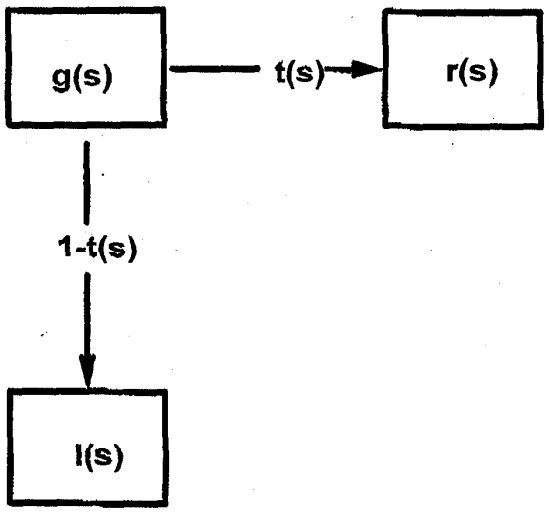

Figure AI- 1: Sediment transport model to develop a lag deposit (see the text for a definition of terms).

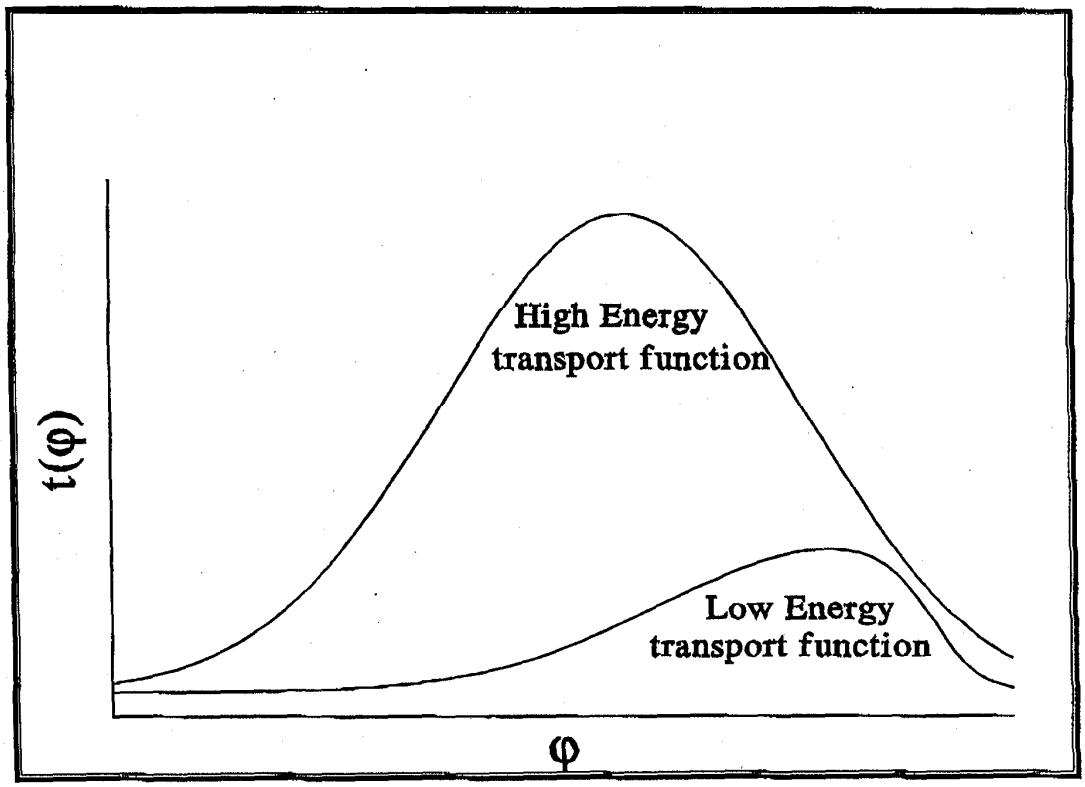

Figure AI- 2: Diagram showing the extremes in the shape of transfer functions t(φ).

The fact that $t(s)$ appears to be mainly a negatively skewed function results in $r(s)$, the sediment in transport, always becoming finer and more negatively skewed than $g(s)$. The function $1\text{-}t(s)$ (Figure AI- 1) is, therefore, positively skewed, with the result that $l(s)$, the lag remaining after $r(s)$ has been removed, will always be coarser and more positively skewed than the original source sediment.

If $t(s)$ is applied to $g(s)$ many times (i.e., n times, where n is large), then the variance of both $g(s)$ and $l(s)$ will approach zero (i.e., sorting will become better). Depending on the initial distribution of $g(s)$, it is mathematically possible for variance to become greater before eventually decreasing. In reality, an increase in variance in the direction of transport is rarely observed.

Given two sediments whose distributions are, $d_1(s)$ and $d_2(s)$, and $d_2(s)$ is coarser, better sorted and more positively skewed than $d_1(s)$, it may be possible to conclude that $d_2(s)$ is a lag of $d_1(s)$ and that the two distributions were originally the same (Case A;Table AI- 1).

1.2 Case B (Sediments becoming finer in the direction of transport)

Consider a sequence of deposits ($d_1(s)$, $d_2(s)$, $d_3(s)$,...) that follows the direction of net sediment transport (Figure AI- 3). Each deposit is derived from its corresponding sediment in transport according to the "3-box model" shown in Figure AI- 1. Each $d_n(s)$ can be considered a lag of each $r_n(s)$. Thus, $d_n(s)$ will be coarser, better sorted and more positively skewed than $r_n(s)$. Similarly, each $r_n(s)$ is acted upon by its corresponding $t_n(s)$ with the result that the sediment in transport becomes progressively finer, better sorted and more negatively skewed. Any two sequential deposits (e.g., $d_1(s)$ and $d_2(s)$) may be related to each other by a function $X(s)$ so that:

$$d_x(s) = k \cdot d_1(s) \cdot X(s)$$

$$\text{or } X(s) = \frac{d_2(s)}{k \cdot d_1(s)} \qquad \text{.....(9)}$$

$$\text{where } k = \frac{1}{\sum_{i=1}^{N} d_1(s_i) \cdot X(s_i)}$$

As illustrated in Figure AI- 3, $d_2(s)$ can also be related to $d_1(s)$ by:

$$d_2(s) = \frac{k \cdot d_1(s) t_1(s)[1 - t_2(s)]}{1 - t_1(s)}$$

$$= k \cdot d_1(s) X(s) \quad (1) \qquad \text{.....(10)}$$

$$\text{where } X(s) = \frac{t_1(s)[1 - t_2(s)]}{1 - t_1(s)} \quad (2)$$

The function $X(s)$ combines the effects of two transfer functions $t_1(s)$ and $t_2(s)$ (Equation 2). It may also be considered as a transfer function in that it provides the statistical relationship between the two deposits and it incorporates all of the processes responsible for sediment erosion, transport and deposition. The distribution of the deposit $d_2(s)$ will,

therefore, change relative to $d_1(s)$ according to the shape of $X(s)$ which, in turn, is derived from the combination of $t_1(s)$ and $t_2(s)$ as expressed in Equation 2. It is important to note that $X(s)$ can be derived from the distributions of the deposits $d_1(s)$ and $d_2(s)$ (Equation 1) and it provides the relative probability of any particular sized grain being eroded from d_1, transported and deposited at d_2.

Using empirically derived $t(s)$ functions, it can be shown that when the energy level of the transporting process decreases in the direction of transport (i.e., $t_2(s_i) < t_1(s_i)$) and both are low energy functions (Figure AI- 4), then $X(s)$ is always a negatively skewed distribution. This will result in $d_2(s)$ becoming finer, better sorted and more negatively skewed than $d_1(s)$. Therefore, given two sediments (d_1 and d_2) where $d_2(s)$ is finer, better sorted and more negatively skewed than $d_1(s)$, it may be possible to conclude that the direction of sediment transport is from d_1 to d_2 (Table AI- 1).

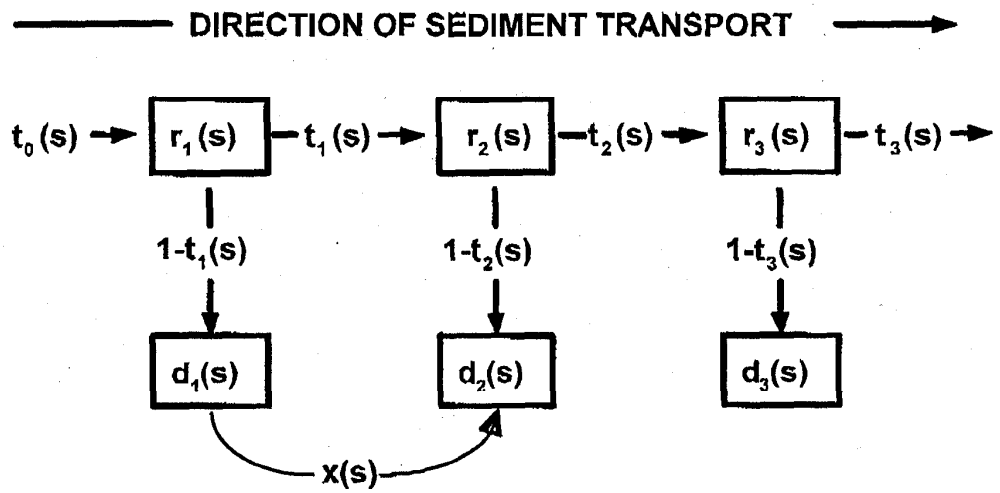

Figure AI- 3: Sediment transport model relating deposits in the direction of transport (see Appendix I for definition of terms).

1.3 1.3 Case C (Sediments becoming coarser in the direction of transport)

In the event that $t_1(s)$ is a high energy function (Figure AI- 2) and $t_2(s_i) < t_1(s_i)$ (i.e., energy is decreasing in the direction of transport), the result of Equation 2 will produce a positively skewed $X(s)$ distribution. Therefore, $d_2(s)$ will become coarser, better sorted and more positively skewed than $d_1(s)$ in the direction of transport (Figure AI- 4). When these changes occur between two deposits, it may be possible to conclude that the direction of transport is from d_1 to d_2 (Table AI- 1).

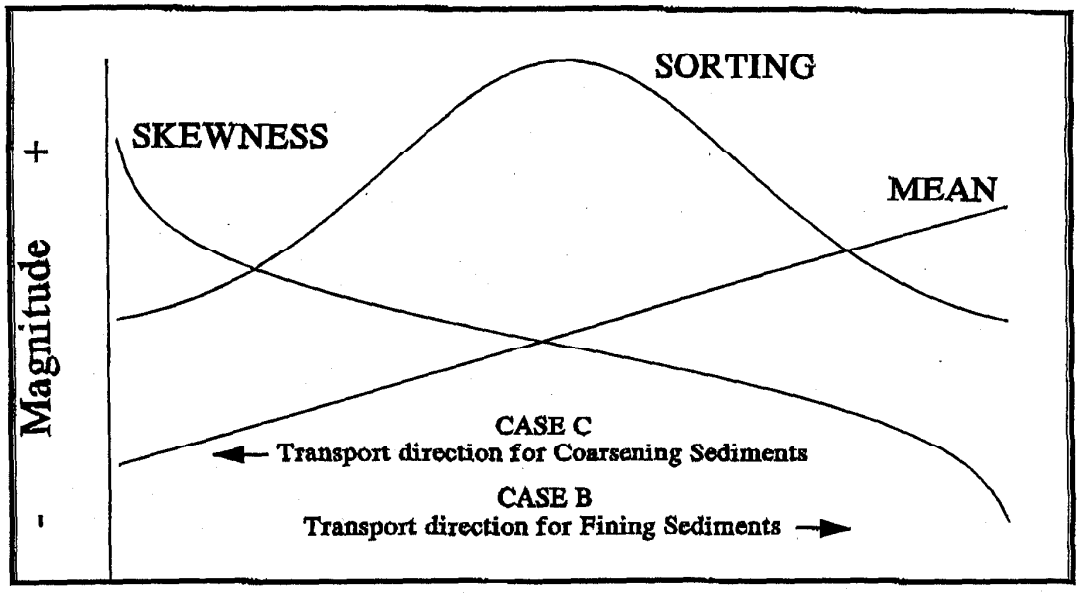

Figure AI- 4: Changes in grain-size descriptors along transport paths.

CASE	RELATIVE CHANGE IN GRAIN-SIZE DISTRIBUTION BETWEEN DEPOSIT d_2 AND DEPOSIT d_1	INTERPRETATION
A	Coarser Better sorted More positively skewed	d_2 is a lag of d_1. No direction of transport can be determined.
B	Finer Better sorted More negatively skewed	(i) The direction of transport is from d_1 to d_2. (ii) The energy regime is decreasing in the direction of transport. (iii) t_1 and t_2 are low energy transfer functions.
C	Coarser Better sorted More positively skewed	(i) The direction of transport is from d_1 to d_2. (ii) The energy regime is decreasing in the direction of transport. (iii) t_1 is a high energy transfer function and t_2 is a high or low energy transfer function (Figure AI- 5).

Table AI- 1: Summary of the interpretations with respect to sediment transport trends when one deposit is compared to another.

Sediment coarsening along a transport path will be limited by the ability of $t_1(s)$ to remain a high energy function. As the deposits become coarser, it will be less and less likely that the transport processes will maintain high energy characteristics. With coarsening, the transfer function will eventually revert to its low energy shape (Figure AI- 2) with the result that the sediment must become finer again.

Cases A and C produce identical grain-size changes between d_1 and d_2 (Table AI- 1). Generally, however, the geological interpretation of the environments being sampled will differentiate between the two Cases.

CASE B: $t_2 < t_1$; both low energy functions

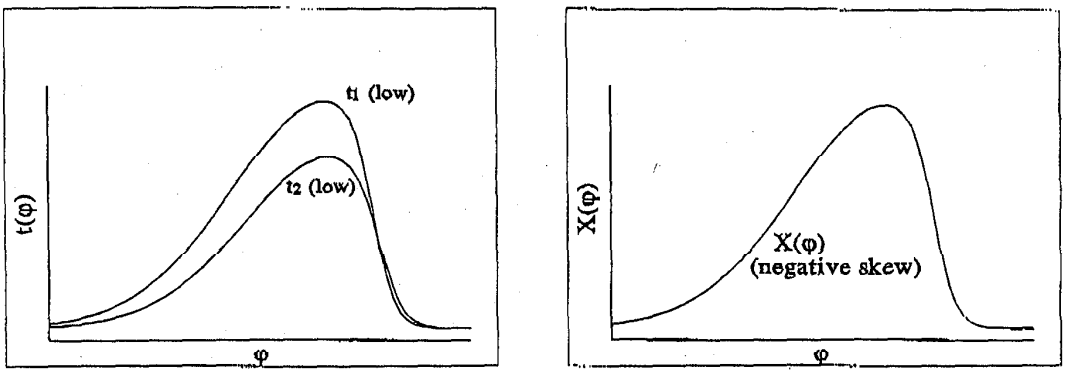

CASE C: $t_2 < t_1$; t_1 is a high energy function; t_2 is high or low.

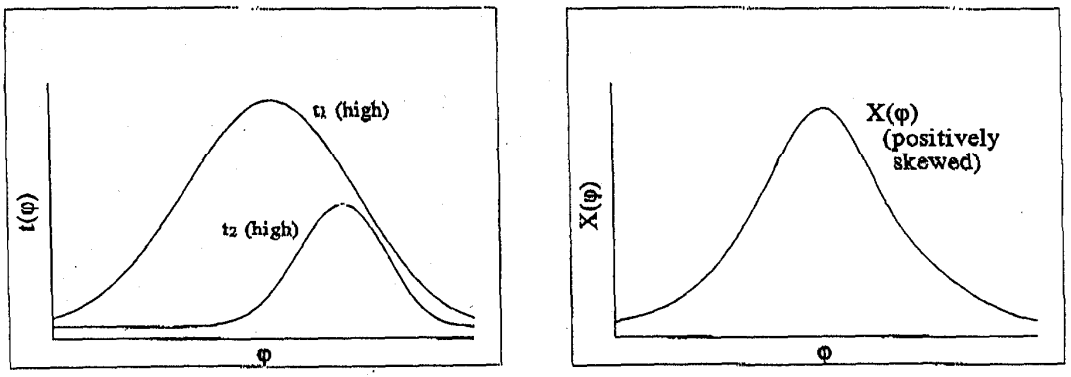

Figure AI- 5: Summary diagram of t_1 and t_2 and corresponding X-distribution (Equation 2) for Cases B and C (Table AI- 1).

2 METHOD TO DETERMINE TRANSPORT DIRECTION FROM GRAIN-SIZE DISTRIBUTIONS (SEDIMENT TREND ANALYSIS)

2.1 Uncertainties

The above model indicates that grain-size distributions will change in the direction of transport according to either Case B or Case C[2] (Table AI- 1; Figure AI- 4). Thus, if any two samples (d_1 and d_2) are compared sequentially (i.e., at two locations within a sedimentary facies), and their distributions are found to change in the described manner, the direction of net sediment transport may be inferred.

A Sediment Trend Analysis attempts to determine the patterns of net sediment transport over an area through the grain-size distributions of the sediments. The sampled sediments are described in statistical terms (by the moment measures of mean, sorting and skewness) and the basic underlying assumption is that processes causing sediment transport will affect the statistics of the sediments in a predictable way. Following from this assumption, the size frequency distributions of the sediments provide the data with which to search for patterns of net sediment transport.

In reality, perfect sequential changes along a transport path as determined by the model are rarely observed. This is because of a variety of uncertainties that may be introduced in sampling, in the analytical technique to obtain grain-size distributions, in the assumptions of the transport model, and in the statistics used in describing the grain-size distributions. These uncertainties may be summarized as follows:

(1) The use of the log-normal distribution:
Although sediments are typically described by a particle weight distribution based on the log of the grain-size (i.e., the phi scale where particle diameter in mm = $2^{-\phi}$) there is, in fact, no way to determine the "best" descriptor for all sediments. The log-normal distribution has been found useful in practice since it appears to highlight important features of naturally occurring sediments. Bias can, however, be introduced in the choice of distribution. For example, the mean of the distribution in phi space is not equal to the mean of the distribution in linear space. Using the moment measures (mean, variance and skewness) may highlight important features and suppress those that are unimportant; however, information will also be lost. There is no way to determine if the lost information is significant (Bowles and McLaren, 1985).

Whatever method is used to describe the sediments, the trend analysis requires the above model which demonstrates that transport processes will change the moment measures of

---

[2] Case A which defines the development of a lag deposit is not used to determine a sediment transport direction. There may be instances when a Case C transport direction is determined which, in fact, is not Case C transport, but rather Case A. For example, in some Arctic environments, sediments become progressively coarser, better sorted and more positively skewed from deep to shallow water. It is impossible to suppose that there is a high energy transport function operating on the deep water sediments resulting in Case C transport towards the shoreline. In this enviroment, ice action and currents result in the winnowing of the finer size fractions as the water shallows. Thus Case A indicating the development of a lag is the accepted Case, rather than Case C. As stated earlier, a geological interpretation may be required to differentiate between the development of a lag (Case A) and a genuine transport pathway (Case C).

sediments in a predictable way. It is hoped that future research may be able to address the possible benefits of using other distributions (e.g., the log hyperbolic distribution; Hartmann and Christiansen, 1992).

(2) Assumptions in the transport model:
In providing a mathematical proof for the transport model used in the Sediment Trend Analysis (McLaren and Bowles, 1985), a basic assumption is made that smaller grains are more easily transported than larger grains. As seen in the transfer functions obtained from flume experiments (Fig. AI-2), this assumption is not strictly true. The curves monotonically increase over only a portion of the available grain sizes before returning to zero. Factors such as shielding whereby the presence of larger grains may impede the transport of smaller grains, or the decreasing ability of the eroding process to carry additional fines with increasing load, demonstrate that the transport process is a complicated function related to the sediment distribution and the strength of the erosion process.

(3) Temporal fluctuations:
Sediment samples may comprise the effects of several transport processes. It is assumed that what is sampled is the "average" of all the transport processes affecting the sample site. The "average" transport process may not conform to the transport model developed for a single transport process.

In a Sediment Trend Analysis, it is assumed that a sample provides a representation of a specific sediment type (or facies). There is no direct time connotation, nor does the depth to which the sample was taken contain any significance provided that the sample does, in fact, accurately represent the facies. For example d_1 may be a sample of a facies that represents an accumulation over several tidal cycles, and d_2 represents several years of deposition. The trend analysis simply provides the sedimentological relationship between the two (see McLaren, 1981 for a more detailed discussion of sampling). The possibility also exists that different samples may result from a different suite of transport events.

(4) Sample spacing:
Sample sites may be too far apart to detect relevant transport processes. With increasing distance between sample locations there is an increasing possibility of collecting sediments unrelated by transport (i.e., different facies). Sample sites placed X m apart can only be reliable to detect transport processes with a spatial scale of 2X m or more. Transport processes with smaller spatial scales may appear as noise or spurious signals.

In practice, selection of a suitable sample spacing takes into account: (1) the number of sedimentological environments likely to be encountered; (2) the desired spatial scale of the sediment trends; and (3) the geographic shape of the study area (see below for further discussion of sample spacing).

(5) Random environmental uncertainties:
All samples will be affected by random errors. These may include unpredictable fluctuations in the depositional environment, the effects of sampling and sub-sampling a representative sediment population, and random measurement errors.

2.2 The use of the Z-score statistic

Given the above list of complicating factors that introduce uncertainties in establishing the net patterns of transport, it is rare to find sequences of samples whose distributions change exactly according to Figure AI- 4. One approach that appears to be successful in determining trends is a simple statistical method whereby the Case (Table AI- 1) is determined among all possible sample pairs contained in a specified sequence. Given a sequence of n samples, there are $\frac{n^2-n}{2}$ directionally orientated pairs that may exhibit a transport trend in one direction, and an equal number of pairs in the opposite direction. When any two samples are compared with respect to their distributions, the mean may become finer (F) or coarser (C), the sorting may become better (B) or poorer (P), and the skewness may become more positive (+) or more negative (-). These three parameters provide 8 possible combinations (Table AI- 2).

	1*	2	3	4
Mean	F	C	F	F
Sorting	B	B	P	B
Skewness	-	-	-	+
	5	**6**	**7****	**8**
Mean	C	F	C	C
Sorting	P	P	B	P
Skewness	+	+	+	-

Table AI- 2: All possible combinations of grain-size parameters

* Case B (Table AI- 1) ** Case A or C (Table AI- 1)

In Sediment Trend Analysis we postulate that a certain relationship exists among the set of n samples, and that this relationship is evidenced by particular changes in sediment size descriptors between pairs of samples. Then the number of pairs for which the trend relationship occurs should exceed the number of pairs that would be expected to occur at random by a sufficient amount for us to state confidently that the trend relationship exists. Suppose the probability of any trend existing between any pair of samples, if the trend relationships were established randomly, is p. Since there are 8 possible trend relationships among 3 sediment descriptors, and we assume that each of these is equally likely to occur, the value of p is set at 0.125.

To determine if the number of occurrences that a particular Case exceeds the random probability of 0.125, the following two hypotheses are tested:

H_0: $p<0.125$, and there is no preferred direction; and
H_1: $p>0.125$, and transport is occurring in the preferred direction.

Using the Z-score statistic in a one-tailed test (Spiegel, 1961), H_1 is accepted if:

$$Z = \frac{x - Np}{\sqrt{Nqp}} \rangle 1.645 \text{ (0.05 level of significance)} \qquad \text{or} \quad \rangle 2.33 \text{ (0.01 level of significance)} \qquad (11)$$

where x is the observed number of pairs representing a particular Case in one of the two opposing directions; and N is the total number of possible unidirectional pairs, given by $\frac{n^2 - n}{2}$. The number of samples in the sequence is n; p is 0.125; and q is $1.0 - p = 0.875$.

The Z statistic is considered valid for $N>30$ (i.e., a large sample). Thus, for this application, a suite of 8 or 9 samples is the minimum required to evaluate adequately a transport direction.

3 DERIVATION OF SEDIMENT TRANSPORT PATHWAYS

From the above it is seen that a variety of uncertainties may preclude obtaining a "perfect" sequence of progressive changes in grain-size distributions from sediment samples that follow a specific transport pathway (Figure AI- 4). In using the Z-score statistic, however, a transport trend may be determined whereby all possible pairs in a sample sequence are compared with each other. When either a Case B or Case C trend exceeds random probability within the chosen sample sequence, the direction of net sediment transport can be inferred. In using the Z-score statistic, a minimum of 9 samples should be used which indicates that, if transport pathways are to be determined over a specific area, a minimum grid of 9 by 9 samples is required (i.e., 81 samples). As suggested above, the grid spacing must be compatible with the area under study and take into account the number of sedimentological environments likely to be involved, the geographic shape of the study area, and the desired statistical certainty of the pathways. For practical purposes, it has been found that, for regional studies in open ocean environments, sample spacing should not exceed 1 km; in estuaries spacing should be reduced to 500 m. For site specific studies (e.g., to determine the transport regime for a single marina), sample spacing will be reduced so that a minimum number of samples can be taken to ensure an adequate coverage (i.e., 9 X 9 samples). Experience has also shown that extra samples should be taken over sites of specific interest (e.g., dredged material disposal sites) and, should the regular grid be insufficient, from specific bathymetric features (e.g., bars and channels).

In determining transport patterns over an area, it is useful to draw an analogy with communication systems. In the latter, information is transmitted to a distant location where a signal is received containing both the desired information as well as noise. The receiver must extract the information from the noisy signal. In theory, the information can be recovered by simply subtracting the noise from the signal, an approach that works well in communications systems because the nature of both the information and the noise is well known.

In sedimentary systems, the information is the direction of net sediment transport, and the received signal is the grain-size distributions of the sediment samples. The goal of a

Sediment Trend Analysis is to extract the information from the noisy signal which, in this case, may be difficult because neither the nature of the information nor the noise is known.

There is, however, another approach that draws from communications theory. In some communications systems, the information from many sources is combined into one signal which, from a statistical viewpoint, is nothing but noise. To extract specific information the receiver assumes that the information is present and determines if that assumption is consistent with the received signal[3].

The same approach may be used in a Sediment Trend Analysis as follows: (i) assume the direction of sediment transport over an area containing many sample sites; (ii) from this assumption, predict the sediment trend that should appear along a particular sequence of samples; (iii) compare the prediction with the actual trend that is derived from the selected samples; and (iv) modify the assumed transport direction and repeat the comparison until the best fit is achieved.

The important feature of this approach is the use of many sample sites to detect a transport direction. This effectively reduces the level of noise. The principal difficulty is that the number of possible pathways in a given area may be too large to mechanize the technique, or to try them all. As a result, the choosing of trial transport directions has, as yet, not been analytically codified (research is on-going to do this). At present, the selection of trial directions is undertaken initially at random; although the term "random" is used loosely in that it is not strictly possible to remove the element of human decision-making entirely. For example, a first look at the possible transport pathways may encompass all north-south, or all east-west directions. As familiarity with the data increases, exploration for trends becomes less and less random. The number of trial trends becomes reduced to a manageable level through both experience and the use of additional information (usually the bathymetry and morphology of the area under study). Following from the communications analogy, when a final and coherent pattern of transport pathways is obtained that encompasses all, or nearly all of the samples, the assumption that there is information (the transport pathways) contained in the signal (the grain-size distributions) has been verified, despite the inability to define accurately all the uncertainties that may be present.

4 THE USE OF R^2

In order to assess the validity of any transport line, we use the *Z*-score and an additional statistic, the linear correlation coefficient R^2, defined as:

$$R^2 = \frac{\sum_i (\hat{y}_i - \bar{y})^2}{\sum_i (y_i - \bar{y})^2}; \text{ where } \hat{y} = f(x_1, x_2, \ldots); \text{ and } \bar{y} = \frac{1}{N}\sum_i y_i \quad \ldots\ldots\ldots\ldots\ldots (12)$$

[3]This is a process referred to as Code Division Multiplexing.

The value of R^2 can range from 0 to 1. The definition of R^2 is based on the use of a model to relate a dependent parameter y to one or more independent parameters $(x_1, x_2, \ldots)$. In our case, the model used is a linear one, which can be written as:

$$\hat{y} = a_o + a_1 \cdot x_1 + a_2 \cdot x_2 \quad \ldots\ldots(13)$$

The data (y, x_1, x_2) are grain-size distribution statistics, and the parameters (a_0, a_1, a_2) are estimated from the data using a least-squares criterion. The dependent parameter is defined as the skewness and the independent parameters are the mean size and the sorting. We make an implicit assumption that grain size samples making up a transport line, if plotted in skewness/sorting/mean space (as in Figure AI- 4), would tend to be clustered along a straight line. The slopes of the straight line, which are the fitted parameters, would depend on the type of transport (fining or coarsening). While there is no theoretical reason to expect a linear relationship among the three descriptors, there is also no theory predicting any other kind of relationship, so using the principle of Occam's Razor[4], we choose the simplest available relationship as our model. High values of R^2 (0.8 or greater) together with a significantly high value of the Z-score give us confidence in the validity of the transport line.

A low R^2 may occur, even when a trend is statistically acceptable for the following reasons: (i) sediments on an assumed transport path are, in reality, from different facies and valid trend statistics occurred accidentally; (ii) the sediments are from a single facies, but the chosen sequence is only a poor approximation of the actual transport path; and (iii) extraneous sediments have been introduced into the natural transport regime, as in the case of dredged material disposal. R^2, therefore, is assessed qualitatively and, when low, statistically acceptable trends must be treated with caution.

5 INTERPRETATION OF THE X-DISTRIBUTION

The shape of the X-distribution is important in defining the type of transport occurring along a line (erosion, accretion, total deposition, *etc.*), and thus the computation of X is important. Let us suppose that we have defined a transport line containing N source/deposit (d_1/d_2) pairs. Then we define X as:

$$X(s) = \sum_{i=1}^{N} \frac{(d_2)_i(s)}{(d_1)_i(s)} \quad \ldots\ldots(14)$$

Often d_2 in one pair is d_1 in another pair, and vice versa. Mean values of d_2 and d_1 are computed through:

$$\bar{d}_1(s) = \sum_{i=1}^{N} (d_1)_i(s); \text{ and } \bar{d}_2(s) = \sum_{i=1}^{N} (d_2)_i(s) \quad \ldots\ldots(15)$$

Note that we do not define X as the quotient of the mean value of d_2 divided by the mean value of d_1, even though the results of the two computations are often almost identical.

---

[4]Occam's Razor: Entities ought not to be multiplied except from necessity. (Occam, 14th Century philosopher, died 1349)

For ease of comparison, d_1, d_2, and X are normalized before plotting in reports, although there is no reason to expect that the integral of the X distribution should be unity.

$X(s)$ may be thought of as a function that describes the relative probability of each particle being removed from d_1 and deposited at d_2. It must be emphasized that the processes responsible for the transport of particles from d_1 to d_2 are unknown; they may in one environment be breaking waves, in another tidal residual currents and, in still another, incorporate the effects of bioturbation.

Examination of X-distributions from a large number of different environments has shown that five basic shapes are most common when compared to the distributions of the deposits $d_1(s)$ and $d_2(s)$ (Fig. AI-6). These are as follows:

(1) Dynamic Equilibrium: The shape of the X-distributions closely resembles $d_1(s)$ and $d_2(s)$. The relative probability of grains being transported, therefore, is a similar distribution to the actual deposits. Thus, the probability of finding a particular sized grain in the deposit is equal to the probability of its transport and re-deposition (i.e., there must be a grain by grain replacement along the transport path). The bed is neither accreting nor eroding and is, therefore, in dynamic equilibrium.

An X-distribution signifying dynamic equilibrium may be found in either Case B or Case C transport suggesting that there is "fine balance" between erosion and accretion. Often when such environments are determined, both Case B and Case C trends may be significant along the selected sample sequence. This is referred to as a "Mixed Case", and when this occurs it is believed that the transport regime is also approaching a state of dynamic equilibrium.

(2) Net Accretion: The shapes of the three distributions are similar, but the mode of X is finer than the modes of $d_1(s)$ and $d_2(s)$. The mode of X may be thought of as the size that is the most easily transported. Because the modes of the deposits are coarser than X, these sizes are more readily deposited than transported. The bed, therefore, must be in a state of net accretion. Net accretion can only be seen in Case B transport.

(3) Net Erosion: Again the shapes of the three distributions are similar, but the mode of X is coarser than the $d_1(s)$ and $d_2(s)$ modes. This is the reverse of net accretion where the size most easily transported is coarser than the deposits. As result the deposits are undergoing erosion along the transport path. Net erosion can only be seen in Case C transport.

(4) Total Deposition I: Regardless of the shapes of $d_1(s)$ and $d_2(s)$, the X-distribution more or less increases monotonically over the complete size range of the deposits. Sediment must fine in the direction of transport (Case B); however, the bed is no longer mobile. Rather, it is accreting under a "rain" of sediment that fines with distance from source. Once deposited, there is no further transport. The occurrence of total deposition is usually confined to cohesive, muddy sediments.

(5) Total Deposition II (Horizontal X-Distributions): Occurring only in extremely fine sediments when the mean grain-size is very fine silt or clay, the X-distribution may be essentially horizontal. Such sediments are usually found far from their source and the horizontal nature of the X-distribution suggests that their deposition is no longer related

strictly to size-sorting. In other words, there is now an equal probability of all sizes being deposited. This form of the X-distribution was first observed in the muddy deposits of a British Columbia fjord and is described in McLaren, Cretney et al., 1993. Because the trends occur in very fine sediments where any changes in the distributions are extremely small, horizontal X-distributions may be found in both Case B and Case C trends.

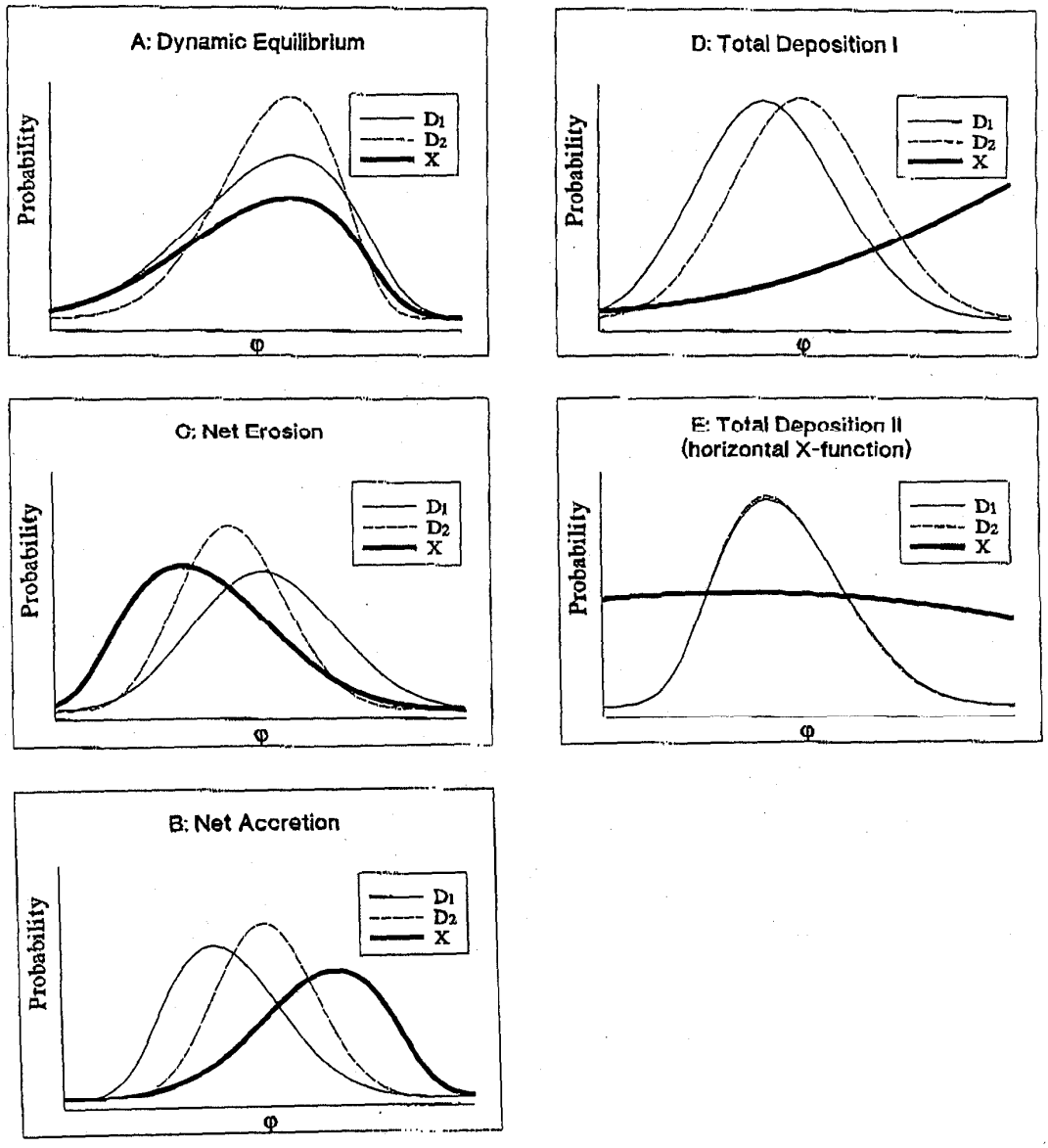

Figure AI- 6: Summary of the interpretations given to the shapes of X-distributions relative to the D1 and D2 deposits.

6 REFERENCES

Bowles, D. and McLaren, P., 1985: Optimal configuration and information content of sets of frequency distributions - discussion; Journal of Sedimentary Petrology, V.55, 931-933.

Hartmann, D., and Christiansen, C., 1992: The hyperbolic shape triangle as a tool for discriminating populations of sediment samples of closely connected origin; Sedimentology, V.39, 697-708.

McLaren, P. and Bowles, D., 1985: The effects of sediment transport on grain-size distributions; Journal of Sedimentary Petrology, V.55, 457-470.

McLaren, P., Cretney, W.J., and Powys, R., 1993: Sediment pathways in a British Columbia fjord and their relationship with particle-associated contaminants; Journal of Coastal Research, V.9, 1026-1043.

McLaren, P., 1981: An interpretation of trends in grain-size measures; Journal of Sedimentary Petrology, V.51, 611-624.

APPENDIX II

Grain-Size Analysis Data

TABLE OF CONTENTS

LIST OF TABLES

1.0 INTRODUCTION

As of April 2000, GeoSea® is using a Malvern Mastersizer 2000 laser particle sizer for the grain-size analysis of sediments. This unit is state-of-the-art equipment. It is extremely accurate, the results are consistent, and it enables the determination of a large range of particle sizes using a single technique[1]. A laser particle sizer is also the most efficient way to analyze the large numbers of samples that are required in Sediment Trend Analysis. This Appendix describes the methodology used in our laboratory.

2.0 METHODOLOGY

2.1 Malvern Mastersizer 2000 laser particle sizer

The instrument is based on the principle of laser diffraction. Light from a low power helium-neon laser is used to form a collimated, monochromatic (red) beam of light which is the analyser beam. The unit also has a solid state blue light source. The shorter wavelength of the blue light allows for greater accuracy in the sub-micron range. Particles from sediment samples enter the beam via a dispersion tank that pumps the material, carried in water, through a sample cell. The resultant light scatter is incident onto the detector lens. The latter acts as a Fourier Transform Lens forming the far field diffraction patterns of the scattered light at its focal plane. Here a custom designed detector in the form of 52 concentric rings gathers the scattered light over a range of solid angles of scatter. When a particle is in the analyser beam its diffraction pattern is stationary and centred on the optical axis of the range lens. Un-scattered light is also focused onto an aperture on the detector. The total laser power exiting the optical system through this aperture enables measurement of the sample concentration.

In practice many particles are simultaneously present in the analyser beam and the scattered light measured on the detector is the sum of all individual patterns overlaid on the central axis. Our instrument is set to take 30,000 such measurements (snaps), which are then averaged to build up a light scattering characteristic for that sample based upon the population of individual particles. Applying the Mie theory of light scattering, the output from the detector is then processed by a computer, generating a final distribution.

Particles scatter light at angles related to their diameter (*i.e.*, the larger the particle, the smaller the angle of scatter and *vice versa*). Over the size range of interest, which is 0.02 micron (μ) and larger for this instrument, scattering is independent of the optical properties of the medium of suspension or the particles themselves. Through a process of constrained least squares fitting of theoretical scattering predictions to the observed data, the computer calculates a volume size distribution that would give rise to the observed scattering characteristics. No *a priori* information about the form of the size distribution

---

[1]Most techniques to measure grain-size distributions require sand to be separated from the finer fractions; different analytical methods are used for each split (e.g., settling tube and sedigraph) and the two distributions are then merged together to obtain a complete distribution. Laser analysis does not require such a split, except when very coarse materials are present (coarse sand to gravel-sized fractions).

is assumed, allowing for the characterization of multi-modal distributions with high resolution.

2.2 Laboratory technique

GeoSea has developed a standard operating procedure (SOP) using the Malvern Mastersizer 2000 laser particle size analyser. This ensures that all parameters and variables will remain consistent throughout sample analysis. The methodology covers the range of sizes normally considered important in sediments, is relatively rapid and requires only small samples. No chemical pre-treatment of the samples is undertaken without prior request[2]. Our priority is to determine the size distribution of the naturally occurring sample.

Prior to every analysis, the Mastersizer 2000 automatically aligns the laser beam, and a background measurement of the suspension medium is taken. Samples are initially well mixed before obtaining a representative sub-sample for analysis. The amount of sediment required is about 2 to 4 grams for sands and 0.5 to 1 gram for silt and clay. Samples are introduced into the dispersion unit by wet sieving through a 1mm mesh, eliminating possible blockage of the pumping mechanism by particles that are too large. Disaggregation of the sample is achieved by both mechanical stirring and mild ultrasonic dispersion in the sample dispersion unit[3]. If material remains on the 1mm sieve then the weight percent for each of the coarse sizes (-2.0ϕ to 0.5ϕ[4]; 4.0mm to 0.7mm) is obtained by dry sieving at 0.5ϕ intervals.

---

[2]Occasionally we are asked to remove organic matter by peroxide digestion, or carbonates by treatment with weak acid.

[3]GeoSea has conducted several experiments concerning the degree of ultrasonic dispersion that is desirable. If no ultrasonic dispersion is used, fine particles tend to remain as relatively large aggregates producing an erroneously coarse sediment distribution. With increasing ultrasonic disaggregation a distribution will tend to become increasingly finer as flocs become broken apart. Total disaggregation of the fine material may be desirable for some purposes, but for Sediment Trend Analysis we find that the flocs are best treated as part of the overall grain-size distribution. This is because flocs form particular sized particles that behave as separate entities in the transport regime, whereas total disaggregation would produce a grain-size distribution containing particle sizes that were not actually behaving independently during their transport and deposition. Although we find that increasing the degree of disaggregation changes the specific parameters of a grain-size distribution, it is insufficient to produce significant changes in the derived sediment trend statistics. The degree of ultrasonic dispersion presently used by GeoSea appears to be adequate to break apart the sediment into its component particle sizes without excessive damage to those sizes composed of flocculated material.

[4]ϕ (phi) is the unit of measure most commonly used in sediment size distributions where $\phi = -\frac{\log(mm)}{\log(2)}$.

Table 1: Grain-size scales for sediments.

U.S. Standard Sieve Mesh Number	Diameter (*mm*)	Diameter (*microns*)	Phi Value	Wentworth Size Class	Sediment Type
5	4.00		-2.00		
6	3.36		-1.75		
7	2.83		-1.50	Granule	GRAVEL
8	2.38		-1.25		
10	2.00		-1.00		
12	1.68		-0.75		
14	1.41		-0.50	Very Coarse Sand	
16	1.19		-0.25		
18	1.00		0.00		
20	0.84	840	0.25		
25	0.71	710	0.50	Coarse Sand	
30	0.59	590	0.75		
35	0.50	500	1.00		
40	0.42	420	1.25		
45	0.35	350	1.50	Medium Sand	SAND
50	0.30	300	1.75		
60	0.25	250	2.00		
70	0.21	210	2.25		
80	0.177	177	2.50	Fine Sand	
100	0.149	149	2.75		
120	0.125	125	3.00		
140	0.105	105	3.25		
170	0.088	88	3.50	Very Fine Sand	
200	0.074	74	3.75		
230	0.0625	62.5	4.00		
270	0.053	53	4.25		
325	0.044	44	4.50	Coarse Silt	
	0.037	37	4.75		
	0.031	31	5.00		
	0.0156	15.6	6.00	Medium Silt	
	0.0078	7.8	7.00	Fine Silt	
	0.0039	3.9	8.00	Very Fine Silt	MUD
	0.002	2	9.00		
	0.00098	0.98	10.00		
	0.00049	0.49	11.00	Clay*	
	0.00024	0.24	12.00		
	0.00012	0.12	13.00		
	0.00006	0.06	14.00		

(* The Clay/Silt boundary is sometimes taken at 2 microns, or 9 phi.)

2.3 Merge method

GeoSea has developed software that allows the dry-sieved weights and measurements from the laser unit to be merged into a final distribution within the range of -2.0ϕ to 15ϕ, in size bins of equal width (0.5 ϕ) in ϕ-space. The results from the Mastersizer 2000 consist of a set of 52 size bins, where the bin width is inversely proportional to the mean particle size in the bin, with the percentage of material in each bin. A summary of the merging process follows:

(1) Sieve data

Sieving is carried out at half-phi intervals from -2.0ϕ to 0.5ϕ. The weights are normalized and the percentage smaller than 0.5ϕ is used to renormalize the Malvern values using the methods described above. The portion of the lens data above 0.5ϕ is removed and replaced with sieve data.

2.4 Presentation of Results

Size distribution data are generally provided as both hard copy (Table 2) and as a PC computer file. The file format is as comma-separated ASCII values (*.csv) in which the data for each sample are contained in a single line. The first line in the file defines the variables and the phi scale, and is followed by the weight percentages for the samples. These files can be easily imported into a Microsoft Excel spreadsheet. The interpretation of the data is as follows: the weight percentage shown under a size heading is the amount of material found in a bin with size boundaries set by the previous size heading as the upper size limit and the current size heading as the lower limit. For example, the weight percent shown under the heading 1.5ϕ is the amount in the bin bounded by 1.0ϕ and 1.5ϕ. Because of the way the file is written the first size fraction in the list (-2.0ϕ) always has zero weight percent.

The hard copy (Table 2) consists of a printout of the data in spreadsheet form and, when requested, plots of each sample showing its histogram and cumulative curve in both phi and micron units.

Wetlands Waterway Sample Attributes
Coords are UTM Zone 10, NAD 83

Sample ID	Easting	Northing	Depth (m)	Type	Mean	Sorting	Skewness	% Gravel	% Sand	% Mud
1	547154.7	5236444.1	12.2	SM	6.158	2.172	-0.355	0.0	28.4	71.6
2	547083.8	5236513.3	12.0	SM	4.812	2.136	-0.129	0.0	35.3	64.7
3	548088.8	5235285.0	12.0	SM	5.044	2.088	-0.21	0.0	30.8	69.2
4	548008.0	5235480.0	12.0	SM	4.811	2.357	-0.151	0.0	38.9	61.1
5	548080.0	[illegible]	10.5	SM	5.566	1.729	-0.121	0.0	20.8	79.2
6	548626.8	5236733.3	11.7	SM	6.103	1.808	-0.12	0.0	28.2	71.8
7	548831.1	5236775.8	2.0	MS	3.816	1.888	0.218	0.0	55.8	44.2
8	548837.8	5236773.7	0.8	MS	3.989	1.759	0.156	0.0	53.8	46.2
9	548740.8	5236008.8	12.5	SM	4.738	2.283	-0.202	0.1	51.7	48.4
10	548851.1	5236032.8	3.1	GS	2.624	2.325	0.589	34.1	48.5	17.5
11	548587.8	5235841.4	3.8	MS	3.882	2.136	0.238	0.1	54.3	45.7
12	548887.4	5236080.9	11.3	SM	6.43	1.904	-0.314	0.1	22.3	77.7
13	548777.1	5235896.4	1.8	MS	2.719	2.135	0.964	0.1	74.9	25.1
14	548477.8	5235920.8	10.4	SM	6.461	1.843	-0.243	0.1	21.8	78.4
15	548684.1	5235861.2	3.5	GS	1.881	2.261	0.754	41.8	47.3	10.9
16	548287.8	5236890.0	6.1	SM	6.317	1.891	-0.217	0.1	24.6	75.4
17	548997.5	5236881.3	10.1	SM	6.327	1.997	-0.298	0.1	24.8	75.2
18	548115.1	5236027.0	5.0	S	1.045	1.798	1.806	13.1	79.5	7.8
19	548208.8	5236029.4	10.7	SM	4.883	2.248	-0.219	0.1	32.8	67.8
20	548288.8	5236088.8	6.1	MS	4.179	2.276	0.217	0.1	50.0	50.0
21	548019.4	5236088.0	9.1	SM	5.031	2.113	-0.188	0.1	31.1	68.9
22	548133.8	5236088.7	10.8	SM	5.858	2.048	-0.198	0.1	30.2	69.8
23	548223.7	5236137.8	1.8	MS	3.871	1.884	0.331	0.1	58.8	41.2

Table 2

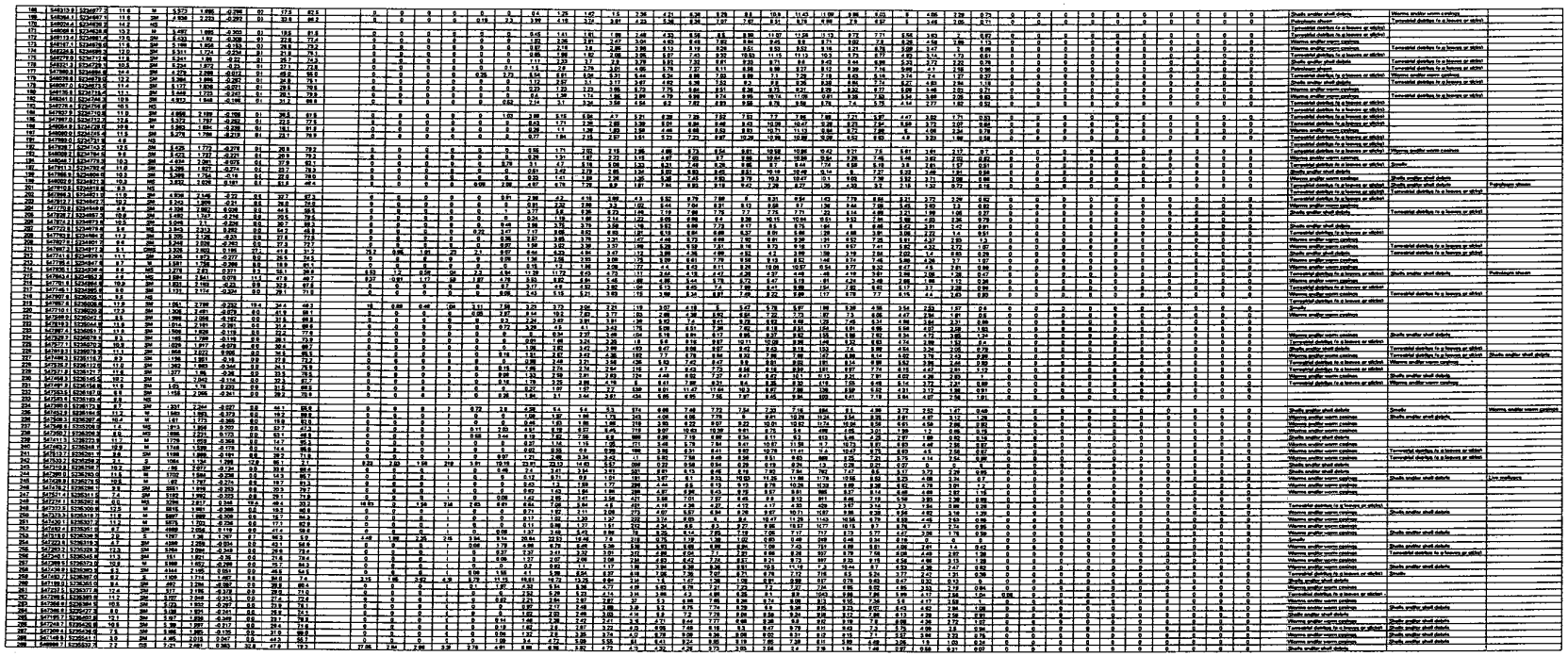

APPENDIX III

Sediment Trend Statistics for All Selected Sample Lines (see Fig. 3)

Definitions:

(i) R^2 = multiple correlation coefficient derived from the mean, sorting and skewness of each sample pair making up a significant trend. This is a relative indication of how well the samples are related by transport.

(ii) Case B: Sediments becoming finer, better sorted and more negatively skewed in the direction of transport.

(iii) Case C: Sediments becoming coarser, better sorted and more positively skewed in the direction of transport.

(iv) N = number of possible pairs in the line of samples.

(v) X = number of pairs making a particular trend in a specific direction.

(vi) X = Z-score statistic: ** are those trends significant at the 99% level. * are those trends significant at the 95% level. (Only trends at the 99% level are accepted.)

(vii) Down = transport in the "down-line" direction.
Up = transport in the "up-line" direction.

(viii) Status defines the dynamic behaviour of the sediments making up the line of samples (i.e., Net Erosion, Net Accretion, Dynamic Equilibrium etc.) See Appendix I for a complete explanation.

Line		R2	N	X	Z	Interpretation
1	B Down:	1.00	6	4	4.01**	Total Deposition I
	Up:		6	1	0.31	
	C Down:		6	0	-0.93	
	Up:		6	1	0.31	
2	B Down:	1.00	15	11	7.12**	Total Deposition I
	Up:		15	3	0.88	
	C Down:		15	0	-1.46	
	Up:		15	1	-0.68	
3	B Down:	0.99	15	8	4.78**	Total Deposition I
	Up:		15	3	0.88	
	C Down:		15	0	-1.46	
	Up:		15	2	0.10	
4	B Down:	0.99	21	13	6.85**	Total Deposition I
	Up:		21	2	-0.41	
	C Down:		21	3	0.25	
	Up:		21	0	-1.73	
5	B Down:	0.98	36	22	8.82**	Total Deposition I
	Up:		36	7	1.26	
	C Down:		36	3	-0.76	
	Up:		36	1	-1.76	
6	B Down:		15	2	0.10	Net Erosion
	Up:		15	1	-0.68	
	C Down:	0.30	15	5	2.44**	
	Up:		15	3	0.88	
7	B Down:		21	0	-1.73	Net Erosion
	Up:		21	4	0.91	
	C Down:	0.95	21	11	5.53**	
	Up:		21	3	0.25	
8	B Down:		21	0	-1.73	Net Erosion
	Up:		21	3	0.25	
	C Down:	0.94	21	8	3.55**	
	Up:		21	6	2.23*	
9	B Down:	0.70	15	7	4.00**	Net Accretion
	Up:		15	0	-1.46	
	C Down:		15	4	1.66*	
	Up:		15	0	-1.46	
10	B Down:	1.00	3	2	2.84**	Net Accretion
	Up:		3	0	-0.65	
	C Down:		3	0	-0.65	
	Up:		3	0	-0.65	
11	B Down:	0.95	45	31	11.44**	Dynamic Equilibrium
	Up:		45	5	-0.28	
	C Down:		45	2	-1.63	
	Up:		45	4	-0.73	

Line		R2	N	X	Z	Interpretation
12	B Down:		36	9	2.27*	Dynamic Equilibrium
	Up:		36	3	-0.76	
	C Down:	0.89	36	16	5.80**	
	Up:		36	3	-0.76	
13	B Down:		55	8	0.46	Net Erosion
	Up:		55	5	-0.76	
	C Down:	0.93	55	33	10.65**	
	Up:		55	3	-1.58	
14	B Down:	0.95	91	24	4.00**	Mixed Case
	Up:		91	8	-1.07	
	C Down:	0.94	91	33	6.85**	
	Up:		91	14	0.83	
15	B Down:	0.93	120	34	5.24**	Mixed Case
	Up:		120	23	2.21*	
	C Down:	0.97	120	42	7.45**	
	Up:		120	10	-1.38	
16	B Down:	0.98	66	38	11.07**	Dynamic Equilibrium
	Up:		66	8	-0.09	
	C Down:		66	1	-2.70	
	Up:		66	4	-1.58	
17	B Down:	0.98	66	32	8.84**	Dynamic Equilibrium
	Up:		66	10	0.65	
	C Down:		66	2	-2.33	
	Up:		66	6	-0.84	
18	B Down:	0.98	55	32	10.24**	Total Deposition I
	Up:		55	9	0.87	
	C Down:		55	6	-0.36	
	Up:		55	5	-0.76	
19	B Down:	0.97	28	12	4.86**	Dynamic Equilibrium
	Up:		28	2	-0.86	
	C Down:		28	7	2.00*	
	Up:		28	4	0.29	
20	B Down:		28	4	0.29	Net Erosion
	Up:		28	5	0.86	
	C Down:	0.99	28	13	5.43**	
	Up:		28	3	-0.29	
21	B Down:		36	6	0.76	Net Erosion
	Up:		36	3	-0.76	
	C Down:	1.00	36	19	7.31**	
	Up:		36	4	-0.25	
22	B Down:	0.91	28	13	5.43**	Total Deposition I
	Up:		28	5	0.86	
	C Down:		28	2	-0.86	
	Up:		28	2	-0.86	

Line		R2	N	X	Z	Interpretation
23	B Down:	0.88	28	18	8.29**	Total Deposition I
	Up:		28	2	-0.86	
	C Down:		28	0	-2.00	
	Up:		28	2	-0.86	
24	B Down:	0.85	36	19	7.31**	Total Deposition I
	Up:		36	2	-1.26	
	C Down:		36	0	-2.27	
	Up:		36	2	-1.26	
25	B Down:	0.98	66	34	9.58**	Total Deposition I
	Up:		66	2	-2.33	
	C Down:		66	0	-3.07	
	Up:		66	11	1.02	
26	B Down:	0.99	55	38	12.69**	Total Deposition I
	Up:		55	4	-1.17	
	C Down:		55	6	-0.36	
	Up:		55	2	-1.99	
27	B Down:	0.88	55	20	5.35**	Total Deposition I
	Up:		55	9	0.87	
	C Down:		55	8	0.46	
	Up:		55	4	-1.17	
28	B Down:	0.71	78	23	4.54**	Total Deposition II
	Up:		78	14	1.46	
	C Down:		78	5	-1.63	
	Up:		78	1	-3.00	
29	B Down:	0.74	91	38	8.44**	Total Deposition II
	Up:		91	7	-1.39	
	C Down:		91	3	-2.65	
	Up:		91	6	-1.70	
30	B Down:	0.70	78	39	10.01**	Total Deposition II
	Up:		78	6	-1.28	
	C Down:		78	3	-2.31	
	Up:		78	2	-2.65	
31	B Down:	0.75	120	53	10.49**	Total Deposition II
	Up:		120	9	-1.66	
	C Down:		120	7	-2.21	
	Up:		120	12	-0.83	
32	B Down:	0.97	45	19	6.03**	Total Deposition II
	Up:		45	8	1.07	
	C Down:		45	7	0.62	
	Up:		45	5	-0.28	
33	B Down:	0.92	210	65	8.09**	Total Deposition II
	Up:		210	35	1.83*	
	C Down:		210	19	-1.51	
	Up:		210	20	-1.30	

Line		R2	N	X	Z	Interpretation
34	B Down:	0.93	66	29	7.72**	Total Deposition II
	Up:		66	14	2.14*	
	C Down:		66	10	0.65	
	Up:		66	2	-2.33	
35	B Down:		6	0	-0.93	Dynamic Equilibrium
	Up:		6	0	-0.93	
	C Down:	1.00	6	3	2.78**	
	Up:		6	2	1.54	

APPENDIX IV

Representative D1, D2 and X-functions

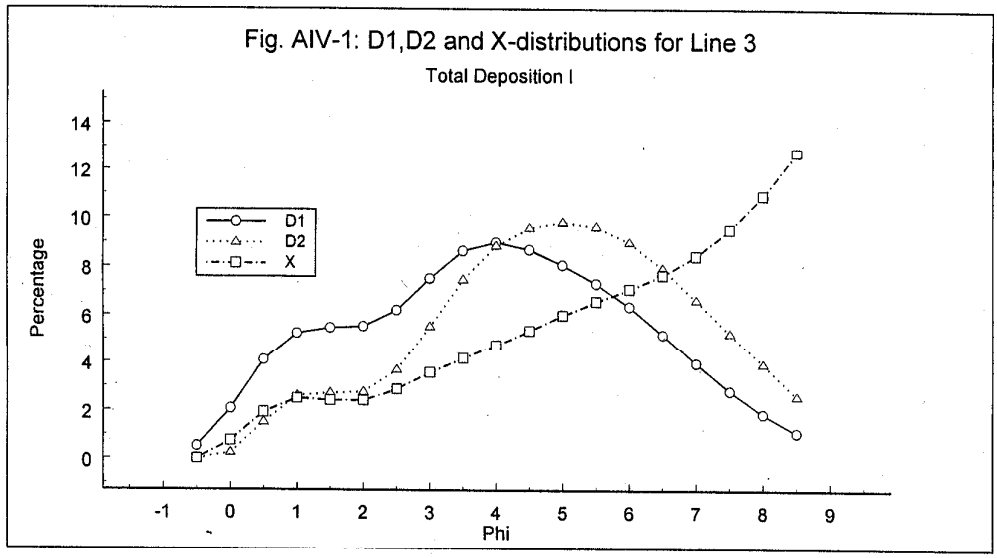
Fig. AIV-1: D1,D2 and X-distributions for Line 3
Total Deposition I
Percentage
Phi
D1
D2
X
14
12
10
8
6
4
2
0
-1
0
1
2
3
4
5
6
7
8
9

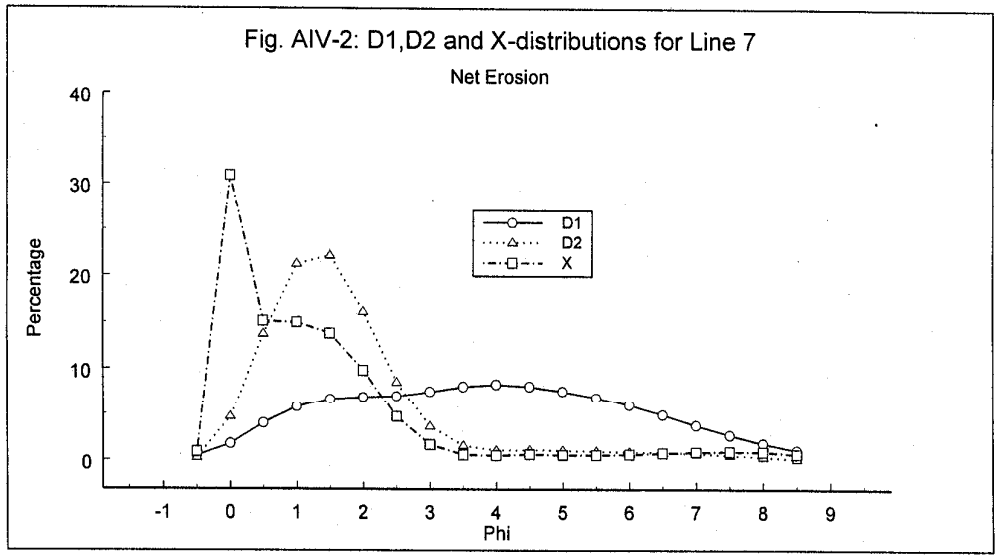
Fig. AIV-2: D1,D2 and X-distributions for Line 7
Net Erosion
Percentage
Phi
D1
D2
X
40
30
20
10
0
-1
0
1
2
3
4
5
6
7
8
9

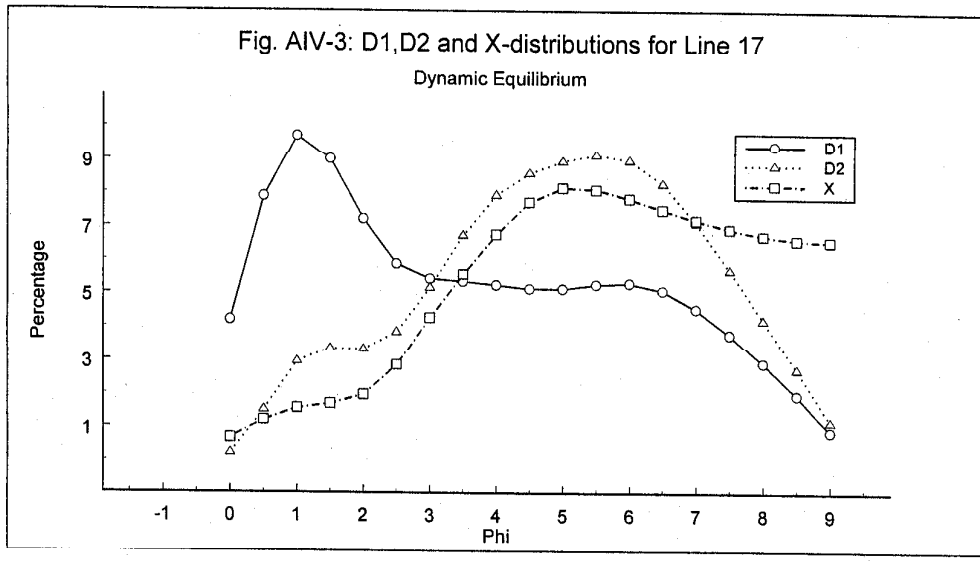
Fig. AIV-3: D1,D2 and X-distributions for Line 17
Dynamic Equilibrium
Percentage
Phi
D1
D2
X
9
7
5
3
1
-1
0
1
2
3
4
5
6
7
8
9

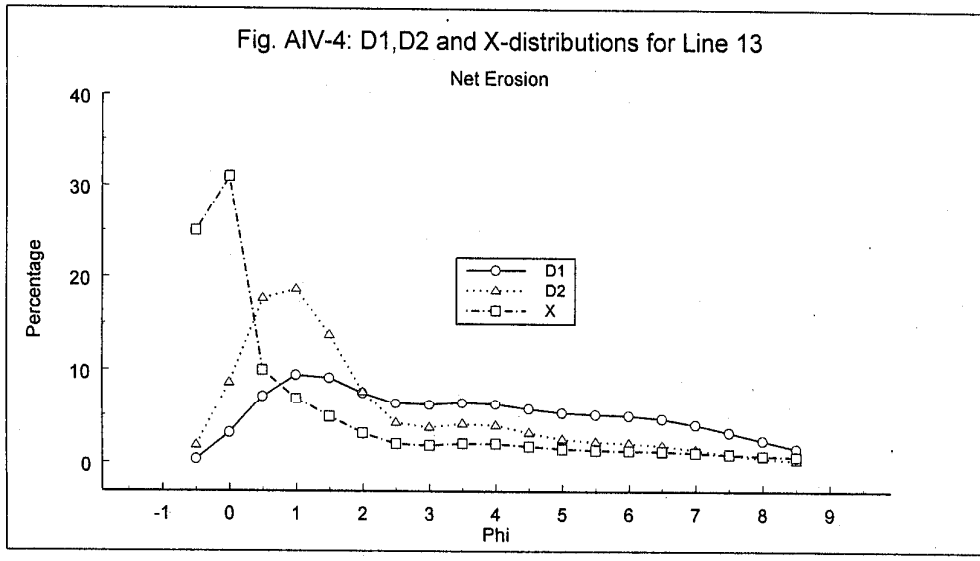
Fig. AIV-4: D1,D2 and X-distributions for Line 13
Net Erosion
Percentage
Phi
D1
D2
X
40
30
20
10
0
-1
0
1
2
3
4
5
6
7
8
9

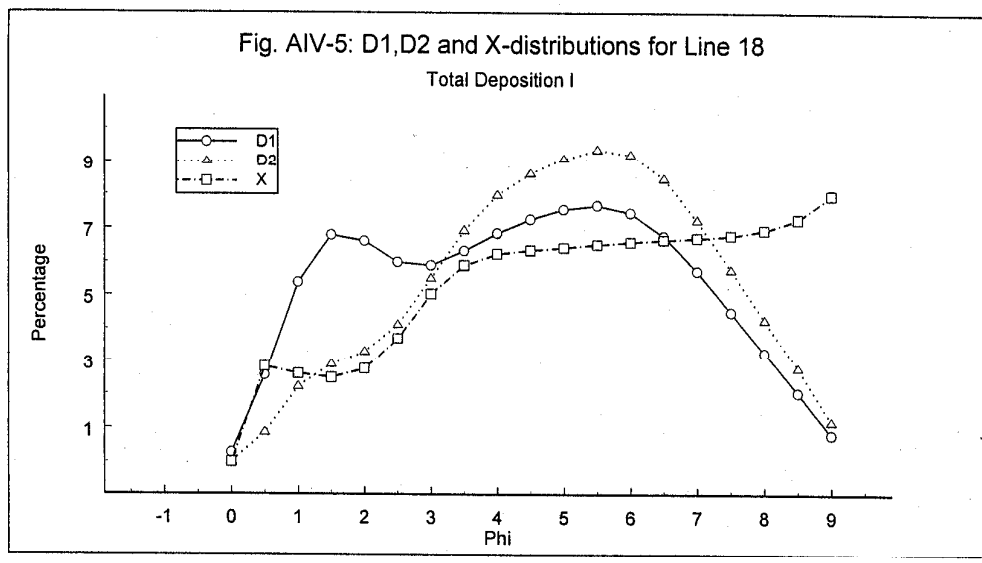
Fig. AIV-5: D1,D2 and X-distributions for Line 18
Total Deposition I
D1
D2
X
Percentage
9
7
5
3
1
-1
0
1
2
3
4
5
6
7
8
9
Phi

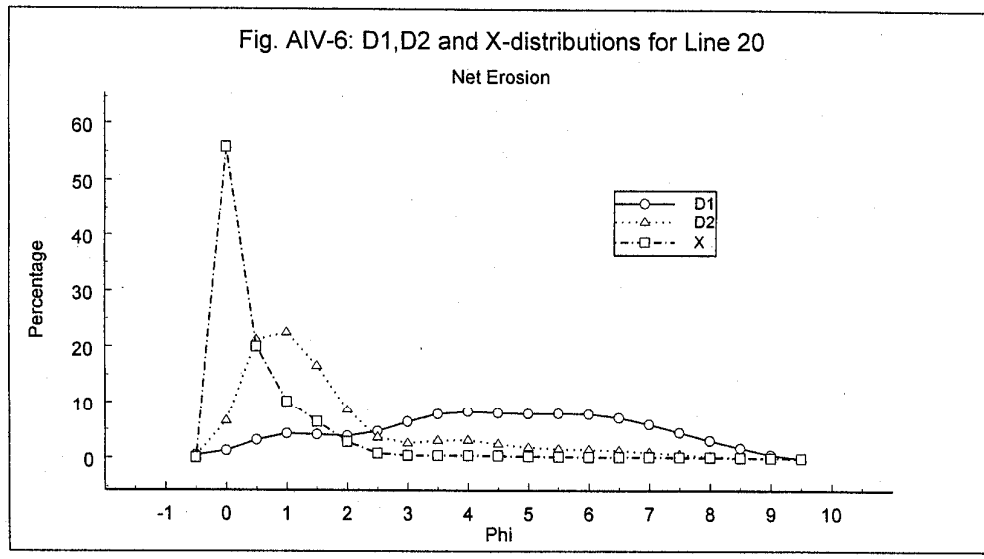
Fig. AIV-6: D1,D2 and X-distributions for Line 20
Net Erosion
D1
D2
X
Percentage
60
50
40
30
20
10
0
-1
0
1
2
3
4
5
6
7
8
9
10
Phi

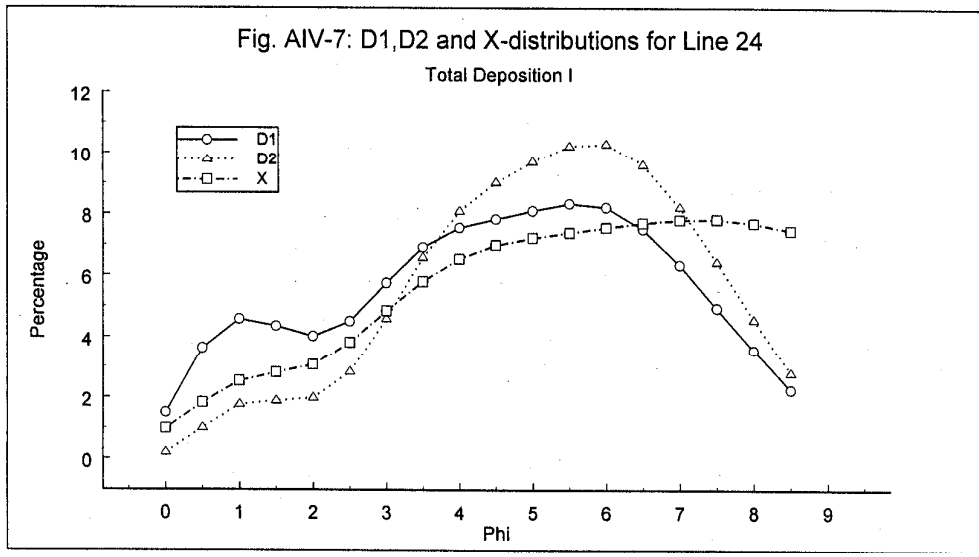
Fig. AIV-7: D1,D2 and X-distributions for Line 24
Total Deposition I
D1
D2
X
Percentage
Phi
0
2
4
6
8
10
12
0 1 2 3 4 5 6 7 8 9

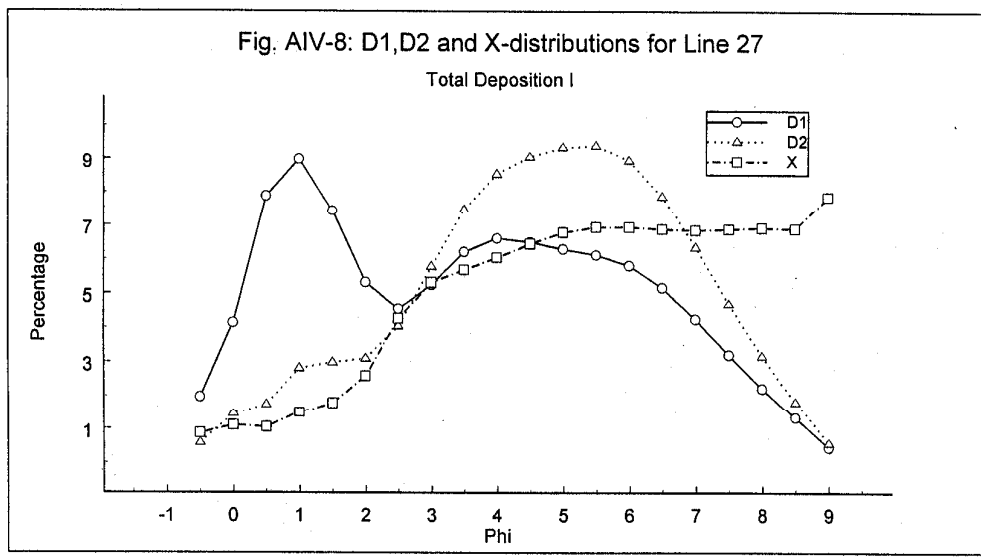
Fig. AIV-8: D1,D2 and X-distributions for Line 27
Total Deposition I
D1
D2
X
Percentage
Phi
1
3
5
7
9
-1 0 1 2 3 4 5 6 7 8 9

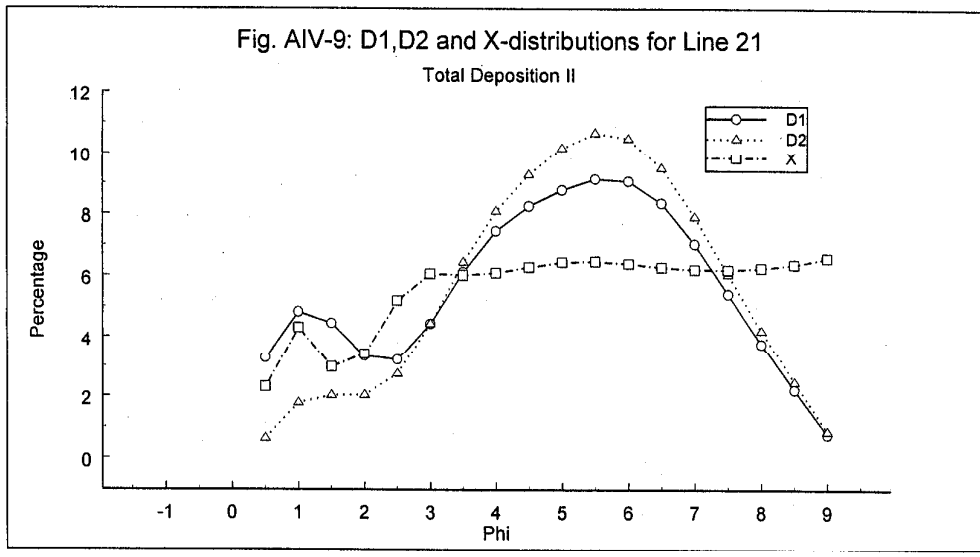
Fig. AIV-9: D1,D2 and X-distributions for Line 21
Total Deposition II
Percentage
Phi
D1
D2
X
12
10
8
6
4
2
0
-1
0
1
2
3
4
5
6
7
8
9

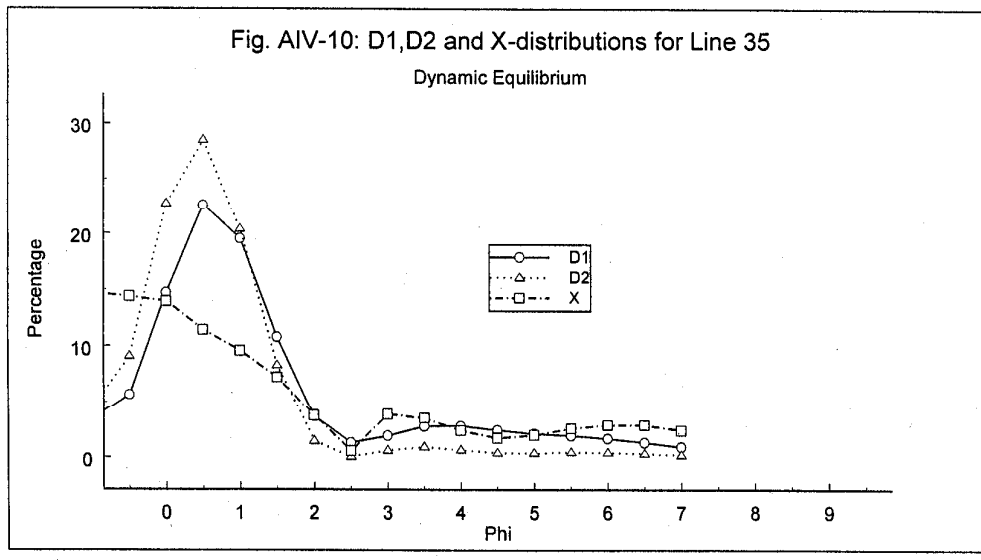
Fig. AIV-10: D1,D2 and X-distributions for Line 35
Dynamic Equilibrium
Percentage
Phi
D1
D2
X
30
20
10
0
0
1
2
3
4
5
6
7
8
9